

## Electron-momentum distribution and spectral function for two holes in finite-cluster $t$ - $J$ models

Robert Eder and Piotr Wróbel\*

*Max-Planck-Institut für Festkörperforschung, 7000 Stuttgart 80, Federal Republic of Germany*

(Received 4 August 1992; revised manuscript received 13 November 1992)

We calculated the momentum distribution and one-particle spectral function for the ground state of two holes in a finite-cluster  $t$ - $J$  model in the framework of the string picture. Previous numerical results for these quantities could be reproduced at least qualitatively. Our interpretation of these data, however, supports a rigid-band approximation starting from the single-hole case rather than a nearest-neighbor hopping band and large Fermi surface. We argue that in order to interpret the finite-cluster data properly, it is crucial to take into account the well-established fact that the ground state of two holes in a finite cluster is a bound state with nontrivial symmetry.

### I. INTRODUCTION

The problem of strongly interacting fermions on a lattice has received considerable attention during the last years. This is because one can hope to gain some insight into the nature of the carriers responsible for high-temperature superconductivity. The simplest model Hamiltonian, which incorporates the key features of the strong correlation limit, is the  $t$ - $J$  Hamiltonian:<sup>1</sup>

$$H = -t \sum_{\langle i,j \rangle, \sigma} (\hat{c}_{i,\sigma}^\dagger \hat{c}_{j,\sigma} + \text{H.c.}) + J \sum_{\langle i,j \rangle} \mathbf{S}_i \cdot \mathbf{S}_j. \quad (1)$$

Here, the  $\mathbf{S}_i$  are the electronic spin operators and the sum over  $\langle i, j \rangle$  stands for a summation over all pairs of nearest neighbors on a two-dimensional square lattice. The operators  $\hat{c}_{i,\sigma}^\dagger$  are expressed in terms of ordinary fermion operators as  $c_{i,\sigma}^\dagger (1 - n_{i,-\sigma})$ .

The problem of a single hole moving through a “background” of spins has been discussed in considerable detail.<sup>2-5</sup> There is general agreement that the dispersion relation is a next-nearest-neighbor hopping band of width  $2J$ , with four degenerate minima at  $(\pm \frac{\pi}{2}, \pm \frac{\pi}{2})$ . This is well understood in terms of the “string” picture, where one assumes that a hole hopping in an antiferromagnetically ordered spin background leaves behind a trace of misaligned spins, which must be repaired by the transverse part of the Heisenberg exchange in order to enable coherent motion. Then, the simplest way to extend this theory to a finite concentration of holes is to assume that the “quasiparticles” may be treated as weakly interacting fermions and to fill up the calculated band (“rigid-band approximation”). One obtains four “hole pockets” around the four degenerate minima of the one-hole dispersion relation. The fraction of the Brillouin zone covered by these pockets equals the hole concentration  $\delta$  and is therefore not consistent with the Luttinger theorem. It seems plausible that similar considerations should apply to the motion of holes in any translationally invariant “spin background” which has sufficiently strong short-range antiferromagnetic correlations (“spin liquid”).

A completely different kind of Fermi surface is predicted by  $1/N$  expansion techniques<sup>6,7</sup> starting from the slave-boson representation of the  $t$ - $J$  model. In this case one obtains a large Fermi surface which is essentially identical to the Fermi surface obtained from the ordinary nearest-neighbor hopping dispersion and which covers a fraction of  $\frac{1-\delta}{2}$  of the total Brillouin zone in agreement with the Luttinger theorem. The width of the nearest-neighbor hopping band, however, is found to scale with the exchange constant  $J$ . Thus, one has two completely different scenarios for the band structure and Fermi surface of the  $t$ - $J$  model in the spin liquid phase: (a) The string picture, together with the rigid-band approximation which predicts a next-nearest-neighbor hopping dispersion and small hole pockets with a total volume of  $\delta$  and (b) the slave-boson mean-field theory would predict a nearest-neighbor-hopping dispersion and a large Fermi surface with a fractional occupancy of the Brillouin zone of  $\frac{1-\delta}{2}$ . Numerical evaluation of the momentum distribution<sup>8-10</sup>  $\langle n_{\mathbf{k},\sigma} \rangle$  and the one-particle spectral function<sup>9</sup> in the ground state of two holes in clusters with 18 and 20 sites (this corresponds to a hole concentration of  $\sim 10$ -12 %) seems to support scenario (b). It is the purpose of the present paper to show that the exact diagonalization data are in fact consistent with the rigid-band picture. The key point is that the ground state of two holes in a finite cluster is a bound state with  $d_{x^2-y^2}$  symmetry. This has a number of consequences, both for the momentum distribution and the spectral function, which apparently have not been realized before.

The plan of the paper is as follows: in Sec. II a variational ansatz for the ground state of a single hole will be sketched. In Sec. III the momentum distribution will be discussed and evaluated using a generalization of the single-hole wave function to obtain an approximate two-hole ground state. In Sec. IV we present a reinterpretation of the spectral function found in Ref. 9, which is based solely on previous exact diagonalization results and elementary symmetry considerations and which implies that the nearest-neighbor hopping band postulated in Ref. 9 does not exist. In Sec. V it is shown that in this

reinterpreted from the data are consistent with the string picture. In the conclusions we summarize the arguments in favor of our interpretation.

At this point, the following remark might be appropriate: there is by now overwhelming experimental evidence that high-temperature superconductors have a Fermi surface which is essentially identical to the one predicted by local-density-approximation calculations. Therefore it may seem not very wise to even think of hole pockets in the  $t$ - $J$  model. The question is, however, if the  $t$ - $J$  model should really reproduce this Fermi surface. After all, if the  $t$ - $J$  model is considered as a simplified version of the large- $U$  Hubbard model, even its exact solution would correspond only to a first-order perturbation treatment of the kinetic term. On the other hand, the Fermi surface found in a noninteracting system is generically a property of precisely the kinetic term and it is unclear if it survives the perturbation treatment of this term. Namely it is the kinetic term that is subject to drastic restrictions in the canonical transformation formalism that leads to the  $t$ - $J$  model. Therefore it might be worth seriously considering the possibility that the  $t$ - $J$  model may by construction be unable to reproduce the large Fermi surface predicted by the Luttinger theorem and therefore we believe that the following calculations are not so unreasonable.

## II. VARIATIONAL WAVE FUNCTION FOR A SINGLE HOLE

It is well known that when a hole is created at a site  $j$  in a Néel-ordered spin state and allowed to hop around, it will feel some “effective potential” due to the formation of “strings”.<sup>11,12</sup> This potential tends to localize the hole around the site  $j$ . Let us denote by  $|j, \nu, \mathcal{P}\rangle$  a state generated by  $\nu$ -fold forward hopping starting from the Néel state with the electron at site  $j$  removed. The symbol  $\mathcal{P}$  denotes a set of numbers which parametrize the geometry of the path the hole has taken. Also we introduce the following decomposition of the  $t$ - $J$  Hamiltonian

$$\begin{aligned} H_{t-J} &= H_0 + H_1, \\ H_0 &= -t \sum_{\langle i,j \rangle, \sigma} (\hat{c}_{i,\sigma}^\dagger \hat{c}_{j,\sigma} + \hat{c}_{j,\sigma}^\dagger \hat{c}_{i,\sigma}) + H_{\text{Ising}}, \\ H_{\text{Ising}} &= J \sum_{\langle i,j \rangle} \left( S_i^z S_j^z - \frac{n_i n_j}{4} \right), \\ H_1 &= \frac{J}{2} \sum_{\langle i,j \rangle} (S_i^+ S_j^- + S_i^- S_j^+). \end{aligned} \quad (2)$$

Then one can make the following ansatz for the ground state of  $H_0$  in the subspace of string states with starting point  $j$ :

$$|\Phi_j\rangle = \sum_{\nu} \alpha_{\nu} \left( \sum_{\mathcal{P}} |j, \nu, \mathcal{P}\rangle \right). \quad (3)$$

The inner sum in this expression runs over all different paths of length  $\nu$  and the coefficients  $\alpha_{\nu}$  are to be determined from the requirement of minimum total energy.

Assuming that the number of frustrated bonds increases linearly with the length of the string and introducing a new function  $\beta_{\nu}$  by  $\beta_{\nu} = \alpha_{\nu}/(z-1)^{\nu/2}$  ( $z=4$  is the number of nearest neighbors) one can show that the  $\beta$ 's can be determined from the discrete version of a one-dimensional Schrödinger equation with a linearly ascending potential:<sup>11,12</sup>

$$-\frac{z}{z-1} \tilde{t} \beta_1 = E_B \beta_0, \quad (4)$$

$$-\tilde{t}(\beta_{\nu+1} + \beta_{\nu-1}) = [E_B - J(\nu + \frac{1}{2})] \beta_{\nu},$$

where  $E_B$  is the “binding energy” of the localized state  $|\Phi_j\rangle$  and  $\tilde{t} = \sqrt{z-1} \cdot t$ .

The  $t$ - $J$  Hamiltonian allows for a number of processes by which the hole can escape from the string potential. The most important one is the truncation of the string by the transverse part of the Heisenberg exchange. Another less important process is hopping along a spiral path as first discussed by Brinkman and Rice.<sup>13,4</sup> With each of these processes one can associate a potential barrier the hole has to penetrate. Namely in each of these processes the number of frustrated bonds first increases and then decreases again. Thus one can see an effective tight-binding Hamiltonian emerge: while moving through the lattice the hole mostly finds itself in localized states like  $|\Phi_j\rangle$  where it is bound to one particular site by the string potential and mostly by means of the string truncation process it can tunnel from one of these localized states to the next one. Obviously these tunneling processes connect only the sites of one sublattice, so the most natural ansatz for the wave function of the hole with momentum  $\mathbf{k}$  is

$$|\Psi(\mathbf{k})\rangle = \sqrt{\frac{2}{N}} \sum_j e^{-i\mathbf{k}\cdot\mathbf{R}_j} |\Phi_j\rangle. \quad (5)$$

Here  $N$  denotes the number of sites in the system and the summation over  $j$  runs over the sites of one sublattice only. The dispersion relation  $E(\mathbf{k})$  for coherent motion can be obtained by forming the expectation value of the full  $t$ - $J$  Hamiltonian with the wave function (5). One finds that the energy is given by<sup>14</sup>

$$E(\mathbf{k}) = E_{\text{Néel}} + 2J + E_B + \epsilon(\mathbf{k}), \quad (6)$$

where  $\epsilon(\mathbf{k})$  is obtained from an “effective” tight-binding Hamiltonian with nonvanishing hopping matrix elements between second- and third-nearest neighbors. The additional shift by  $J$  is due to the four broken bonds, which cost an energy of  $\frac{J}{2}$  each. It turns out<sup>14</sup> that this simple formalism can reproduce the results of finite-size diagonalizations<sup>15,16</sup> and other numerical methods<sup>4,5,17</sup> with remarkable accuracy. Such a description might be viewed as the  $t$ - $J$  version of the spin-bag concept proposed by Schrieffer *et al.*<sup>18</sup>.

## III. MOMENTUM DISTRIBUTION

First we discuss the momentum distribution, i.e., the ground-state expectation value of the operator

$$n_{\mathbf{k},\sigma} = c_{\mathbf{k},\sigma}^\dagger c_{\mathbf{k},\sigma} = \frac{1}{N} \sum_{j,j'} e^{-i\mathbf{k}\cdot(\mathbf{R}_j - \mathbf{R}_{j'})} c_{j',\sigma}^\dagger c_{j,\sigma}. \quad (7)$$

The momentum-distribution function found by numerical calculations for the  $t$ - $J$  model<sup>8–10,19</sup> usually shows the following features (see for example Fig. 1 of Ref. 9): it is larger inside of the Fermi surface evaluated from the unconstrained hopping term  $H_t = -t \sum_{\langle i,j \rangle, \sigma} (c_{i,\sigma}^\dagger c_{j,\sigma} + \text{H.c.})$  for the half-filled band than outside. For more than one hole in the cluster no indication of “hole pockets” has ever been seen. At first sight, this finding clearly rules out the rigid band picture, but one can deduce from very simple arguments that precisely such a kind of momentum distribution is to be expected also within this scenario.

First, in any system, where the kinetic energy is given by a nearest-neighbor hopping term, the expectation value of the kinetic energy can be expressed in terms of the spin-summed momentum distribution  $n_{\mathbf{k}} = \sum_{\sigma} \langle n_{\mathbf{k},\sigma} \rangle$  as follows:

$$\langle H_t \rangle = -t \sum_{\mathbf{k} \in \text{BZ}} \gamma(\mathbf{k}) n_{\mathbf{k}}, \quad (8)$$

where  $\gamma(\mathbf{k}) = 2[\cos(k_x) + \cos(k_y)]$ . Using  $\gamma(\mathbf{k}) = -\gamma(\mathbf{k} + \mathbf{Q})$ , where  $\mathbf{Q} = (\pi, \pi)$  is the antiferromagnetic wave vector, the sum over momenta can be restricted to the magnetic Brillouin zone, i.e.,

$$\langle H_t \rangle = -t \sum_{\mathbf{k} \in \frac{1}{2}\text{BZ}} \gamma(\mathbf{k})(n_{\mathbf{k}} - n_{\mathbf{k}+\mathbf{Q}}). \quad (9)$$

Taking into account, that  $\gamma(\mathbf{k})$  is positive throughout the magnetic Brillouin zone, one can conclude that in order for the expectation value of the kinetic energy to be negative (as it has to be), the average of  $(n_{\mathbf{k}} - n_{\mathbf{k}+\mathbf{Q}})$  over the magnetic Brillouin zone must be positive; in other words,  $n_{\mathbf{k}}$  must be larger inside the Fermi surface of the half-filled, noninteracting band than outside. In addition  $\gamma(\mathbf{k})$  has its maximum value in the center of the Brillouin zone, so that it is most advantageous to make the difference  $n_{\mathbf{k}=(0,0)} - n_{\mathbf{k}=(\pi,\pi)}$  the largest one. Thus any reasonable theory of the  $t$ - $J$  model must produce the general shape of the momentum distribution found in exact diagonalizations (it is interesting to note that this is independent of possible antiferromagnetic order in the system: the momentum distribution cannot resemble the broken symmetry because otherwise the expectation value of the kinetic energy would vanish, which must be wrong). Observing such an overall shape of  $\langle n_{\mathbf{k},\sigma} \rangle$  on a finite (and rather coarse) mesh of  $\mathbf{k}$  points does therefore not allow conclusions on the existence or location of a Fermi surface defined as a line of discontinuity in the momentum distribution. The most obvious counterexample is the mean-field spin-density-wave ground state of the Hubbard model. It shows the same overall shape of the momentum distribution [see Eq. (9) and Fig. 6 in Ref. 20] but no Fermi surface.

Let us now discuss the string wave function (5) in the light of these considerations. From exact diagonalization studies for a single hole<sup>15</sup> it is known that the spin- $\frac{1}{2}$

spin-bag-type ground state described by this wave function can compete successfully with the Nagaoka-type ferromagnetic state (which gives the optimum value of the kinetic energy) for ratios of  $t/J$  up to  $\simeq 20$ . Thus despite the small coherent bandwidth  $\sim 2J$  this wave function must give an appreciable expectation value of the kinetic energy and hence must have an appreciable variation of  $n_{\mathbf{k}}$  over the Brillouin zone. By inspection of the expression for the energy, Eq. (6), one can see that the only term which can account for this large kinetic energy is  $E_B$ , the “binding energy” of the state  $|\Phi_j\rangle$ . Thus the variation in  $\langle n_{\mathbf{k},\sigma} \rangle$  must be due to the rapid motion of the hole “inside of” the spin bag and straightforward evaluation shows that this is indeed the case. Namely, in a preceding paper<sup>21</sup> it has been shown that the momentum distribution function for a single-hole state like (5) with  $S_z = -\frac{1}{2}$  can be written as

$$\begin{aligned} \langle \Psi(\mathbf{k}_0) | n_{\mathbf{k},\uparrow} | \Psi(\mathbf{k}_0) \rangle &= \left( \frac{1}{2} - \frac{1}{N} \right) \\ &\quad - \frac{\alpha_0^2}{2} \left( \delta_{\mathbf{k},\mathbf{k}_0} + \delta_{\mathbf{k},\mathbf{k}_0+\mathbf{Q}} - \frac{2}{N} \right) \\ &\quad + \frac{\text{const}}{N} \gamma(\mathbf{k}). \end{aligned} \quad (10)$$

The various terms in this expression have different physical interpretations: the first term corresponds to the total number of electrons and is a constant for different values of  $t/J$ . The second term is the contribution from the “center of gravity motion” of the quasiparticle. It is proportional to  $\alpha_0^2$ , which is quite reasonable because this is the weight of the “string of length zero,” i.e., the bare hole in the wave function (5) as can be seen from (3).  $\frac{\alpha_0^2}{2}$  is also the simplest estimate for the pole strength of the quasiparticle peak,<sup>21</sup> so the discontinuity in the momentum distribution at the “Fermi surface” (which encloses only  $\mathbf{k}_0$ ) is equal to the strength of the quasiparticle pole, as it has to be.

The third term has two notable features: it does not resemble the broken symmetry of the wave function (5) and it is independent of the “quasiparticle momentum”  $\mathbf{k}_0$ . This term originates from the rapid motion of the hole inside of the function  $|\Phi_j\rangle$  or, stated differently, the incoherent hole motion inside the spin bag. Namely the momentum distribution operator (7) has matrix elements between any string of length  $\mu$  and other string states of length  $\nu \pm 1$ . Then in Eq. (7)  $j$  and  $j'$  must be nearest neighbors, and therefore the  $\mathbf{k}$  dependence is given by the nearest-neighbor tight-binding harmonic  $\gamma(\mathbf{k})$ . Upon insertion into (8) this term must give the expectation value of the kinetic energy, which can be expressed as

$$\langle H_t \rangle = t \partial_t E_B. \quad (11)$$

This can be verified using the expressions given in Ref. 21. The term which stems from the “center of gravity motion” gives no contribution in (8). This is reasonable, because the delocalization of the hole is mainly due to the “string truncation process,” which involves the Heisenberg exchange and should therefore contribute to the expectation value of this term. From (10) one gets

the clear prediction that the expectation value of the kinetic energy be independent of the total momentum  $\mathbf{k}_0$ . This is readily confirmed by exact diagonalizations: by inspection of Tables II and III of Ref. 22 one can see that the expectation value of the kinetic energy for the lowest single-hole state is to good approximation independent of the total momentum.

From (10) one would expect that for a single hole there are still hole pockets at the ground-state momentum, although the magnitude of the discontinuity is substantially smaller than 1 (numerical evaluation shows that for example at  $t/J = 3$  one has  $\frac{\alpha_0^2}{2} \simeq 0.12$ ). It should be noted that the momentum distribution function for a single hole in a finite cluster<sup>23</sup> is in agreement with (10).

On the other hand, for two holes in the cluster one cannot expect to see such pockets any more. This is due to the well-established fact<sup>22,24-26</sup> that two holes in a finite-cluster  $t$ - $J$  model always form a bound (or at least strongly interacting) state. A bound state of two “quasiparticles” with zero momentum and spin should be written

$$|\Psi_0\rangle = \sum_{\mathbf{k}} \Delta(\mathbf{k}) a_{\mathbf{k},\uparrow}^\dagger a_{-\mathbf{k},\downarrow}^\dagger |0\rangle, \quad (12)$$

where  $\Delta(\mathbf{k}) = \Delta(-\mathbf{k})$ . Evaluating the momentum distribution function of the quasiparticles in this wave function one finds

$$\langle \Psi_0 | a_{\mathbf{k},\sigma}^\dagger a_{\mathbf{k},\sigma} | \Psi_0 \rangle = |\Delta(\mathbf{k})|^2. \quad (13)$$

Therefore  $\langle n_{\mathbf{k},\sigma} \rangle$  will in general be spread out over the whole Brillouin zone and there will be no discontinuity. Strictly speaking the very concept of a Fermi surface is meaningless in a bound state.

To be more quantitative we need to have a reasonably accurate approximation for the two-hole ground-state wave function. To that end, let us first define “two-string states”.<sup>27</sup> We start with a state where two holes have been created independently in the Néel state at the sites  $m, n$  and consider the subspace of states obtained by repeated application of the hopping term. Generalizing Eq. (3) one can write down the following ansatz for the ground state of  $H_0$  within this subspace:

$$|\Phi_{m,n}\rangle = \sum_{\mu,\nu} \alpha_{\mu,\nu} \sum_{\mathcal{P},\mathcal{P}'} |m, n, \mu, \nu, \mathcal{P}, \mathcal{P}'\rangle. \quad (14)$$

Here  $|m, n, \mu, \nu, \mathcal{P}, \mathcal{P}'\rangle$  denotes a state obtained by creating two holes in the Néel state at sites  $m, n$  and letting the hole at  $m$  hop  $\mu$  times and the other one  $\nu$  times. The symbols  $\mathcal{P}, \mathcal{P}'$  denote two sets of numbers which parametrize the geometries of the paths the two holes have taken. An important point is that in the ansatz Eq. (14) the summation over the different paths (as described by the symbols  $\mathcal{P}, \mathcal{P}'$ ) will be restricted to “irreducible states”. The definition of an irreducible state is as follows: a state  $|m, n, \mu, \nu, \mathcal{P}, \mathcal{P}'\rangle$  which has been created by hopping is called an “irreducible state with starting points  $m$  and  $n$ ” if it is not possible to generate the same state with fewer hops starting from a state where the holes have been created at other sites. This definition

as well as its physical meaning was discussed in detail in Ref. 27.

Throughout the remainder of the calculations it will be assumed that the two removed electrons have opposite spins. Thus  $m, m'$  will always denote spins on the up sublattice whereas  $n, n'$  will always denote sites on the down sublattice. Since one is dealing with more than one hole one also has to consider the statistics of the particles. Therefore in all that follows it will be assumed that the “initial state” for the construction of  $|\Phi_{m,n}\rangle$  is always the state  $c_{m,\uparrow} c_{n,\downarrow} |\Phi_{\text{Néel}}\rangle$ .

The coefficients  $\alpha_{\mu,\nu}$  in Eq. (14) should be determined variationally in such a way that the state  $|\Phi_{m,n}\rangle$  is the ground state of  $H_0$  in the subspace of irreducible states with starting points  $m, n$ . Then, the state  $|\Phi_{m,n}\rangle$  might be called a state with two spin bags sitting at the sites  $m$  and  $n$ . In the following we will be exclusively concerned with the case that  $m$  and  $n$  are nearest neighbors. Using analogous approximations as in the derivation of the Eqs. (4) and introducing  $\beta_{\mu,\nu} = \alpha_{\mu,\nu} / (\sqrt{z-1})^{\mu+\nu}$  one can show<sup>27</sup> that this latter function has to obey the following set of difference equations:

$$\begin{aligned} & -\tilde{t}(\beta_{\mu+1,\nu} + \beta_{\mu,\nu+1} + \beta_{\mu-1,\nu} + \beta_{\mu,\nu-1}) \\ & = \left( E'_B - \frac{J}{2} [(z-2)(\mu+\nu) + 1 - \delta_{\mu,0}\delta_{\nu,0}] \right) \beta_{\mu,\nu}. \end{aligned} \quad (15)$$

$E''_B$  is the ground-state energy of  $H_0$  in the subspace of irreducible states with starting points  $m, n$  and it is understood that  $\beta$ 's with a negative index are to be set equal to zero. Equation (15) can be solved numerically.

Next, from exact diagonalization studies,<sup>26,22,24,28</sup> it is known, that the ground state of two holes in 16- and 18-site clusters is a bound state of  $d_{x^2-y^2}$ -type symmetry. Thus, the simplest ansatz for a tightly bound two-hole state with the proper symmetry is

$$\begin{aligned} |\Psi_d\rangle &= \sqrt{\frac{2}{N}} \sum_{m \in A} \frac{1}{2} ( |\Phi_{m,m+\hat{x}}\rangle + |\Phi_{m,m-\hat{x}}\rangle \\ & \quad - |\Phi_{m,m+\hat{y}}\rangle - |\Phi_{m,m-\hat{y}}\rangle ) \\ &= \frac{1}{\sqrt{2N}} \sum_{m \in A, n} \epsilon_{m,n} |\Phi_{m,n}\rangle, \end{aligned} \quad (16)$$

where  $A$  denotes the up sublattice and  $\epsilon_{m,n}$  is equal to 1 if  $m$  and  $n$  are nearest neighbors in the  $x$  direction, equal to  $-1$  if they are nearest neighbors in the  $y$  direction, and zero in all other cases. It has been shown by Dagotto and Schrieffer<sup>28</sup> that a wave function of this type is a good approximation for the two-hole ground state. Next, we insert everything:

$$\langle \Psi_d | n_{\mathbf{k},\sigma} | \Psi_d \rangle = \frac{1}{2N^2} \sum_{m,n,m',n',j,j'} e^{-i\mathbf{k}\cdot(\mathbf{R}_j - \mathbf{R}_{j'})} \langle \Phi_{m',n'} | c_{j',\sigma}^\dagger c_{j,\sigma} | \Phi_{m,n} \rangle \epsilon_{m,n} \epsilon_{m',n'}. \quad (17)$$

There will be quite a number of different contributions to this expression. First, one can always choose  $j = j'$ . This means that one is simply counting the number of spin- $\sigma$  electrons and the result is

$$\delta \langle n_{\mathbf{k},\sigma} \rangle = \frac{1}{2} - \frac{1}{N}. \quad (18)$$

Next, let us consider what is the analog of the contribution which for a single hole described the motion of the “center of gravity” of the spin bag. One process which gives an analogous contribution is shown in Fig. 1. In this process one has  $j = n'$ ,  $j' = n$  and consequently the phase factor is  $e^{-i(k_x - k_y)}$ . The process connects two “double strings” of length 0, which each have the expansion coefficient  $\alpha_{0,0} = \beta_{0,0}$ . There is one minus sign from the product of the  $\epsilon_{m,n}$  and a second one from fermion anti-commutation relations (it is a hole that is moved) Namely the state in Fig. 1(a) reads  $c_{m,\uparrow} c_{n,\downarrow} | \Phi_{\text{Néel}} \rangle$ . By acting with  $c_{n,\downarrow}^\dagger c_{n',\downarrow}$  it is transformed into  $-c_{m,\uparrow} c_{n',\downarrow} | \Phi_{\text{Néel}} \rangle$ , i.e., there is a minus sign due to Fermi statistics. All in all, the prefactor is  $(-1)^2 \beta_{0,0}^2$ . By analogous reasoning, for the process shown in Fig. 2 one obtains a contribution of  $-\beta_{0,0}^2 e^{2ik_y}$ . Summing over all symmetry-equivalent processes one obtains

$$\delta \langle n_{\mathbf{k},\sigma} \rangle = -\frac{1}{2N} \frac{1}{\langle \Psi_d | \Psi_d \rangle} \beta_{0,0}^2 [ \cos(2k_x) + \cos(2k_y) - 4 \cos(k_x) \cos(k_y) ]. \quad (19)$$

Thereby the expression within the brackets is just the square of the Fourier transform of the “real-space wave function”  $\Phi(\mathbf{R}_m - \mathbf{R}_n) = \epsilon_{m,n}$ . Finally, the same process is possible if the hole sitting at site  $m$  in Figs. 1 and 2 has hopped an arbitrary number of hops away from this site without crossing the site  $n'$ . This can be taken into account by replacing

$$\beta_{0,0}^2 \rightarrow c_0 = \beta_{0,0}^2 + \frac{z-2}{z-1} \sum_{\nu=1}^{\infty} \beta_{0,\nu}^2. \quad (20)$$

To see the consequence of this contribution, let us con-

sider the value of the square bracket for some highly symmetric  $\mathbf{k}$  points. Obviously for  $\mathbf{k} = (0,0)$ ,  $(\pi,\pi)$ ,  $(\frac{\pi}{2}, \frac{\pi}{2})$  this contribution is  $-2$  whereas, for  $\mathbf{k} = (\pi,0)$  it is  $+4$ . This explains the finding of Stephan and Horsch,<sup>9</sup> that in the 20-site cluster the value of  $\langle n_{\mathbf{k}} \rangle$  is smaller at  $\mathbf{k} = (\pi,0)$  than at the ground-state momentum of a single hole, which is  $(\frac{\pi}{5}, \frac{3\pi}{5})$ . This redistribution of the holes, however, is due to their mutual interaction and is not the consequence of the formation of a “large” Fermi surface (it should be noted that such a strong redistribution of the holes due to their interaction is by no means implausible, because the dispersion relation for a single hole is almost degenerate on the surface of the magnetic Brillouin zone). This interpretation is confirmed by the work of Poilblanc and Dagotto.<sup>29</sup> Namely one way of interpreting the contribution (19) is that in the bound-state wave function  $|\Psi_d\rangle$  those states have the largest weight, where the two quasiparticles have momenta  $\pm(\pi,0)$  or  $\pm(0,\pi)$  (this was also found previously in an analytic treatment of the ground state of two holes in the  $t$ - $J$  model, see Ref. 27). This in turn is consistent with the results of Poilblanc and Dagotto,<sup>29</sup> who found that the matrix element between the two-hole ground state and a state obtained by creating a second hole in a single-hole state is sharply peaked, when the initial (single-hole) momentum is  $(\pi,0)$  and the momentum of the added hole  $(-\pi,0)$ . In the momentum distribution of the bare electrons, however, this trend is strongly suppressed because of the small overlap of the “spin bag” with the bare hole (as exemplified by the small quasiparticle pole strengths  $\sim 0.1$ ), so that “deep” pockets at  $(\pi,0)$  cannot be observed. Thus the present interpretation reconciles in a simple way the apparently contradicting results of Stephan and Horsch and Poilblanc and Dagotto.

In addition to the contribution discussed previously, there will again be a contribution from the hole motion inside of the two spin bags which upon insertion into (8), must give the expectation value of the kinetic energy. These contributions are discussed in Appendix A. One finds again a contribution

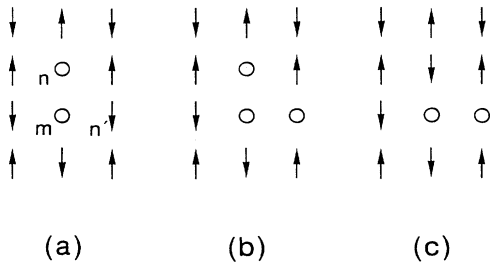


FIG. 1. A process that contributes to  $\langle n_{\mathbf{k},\downarrow} \rangle$ .

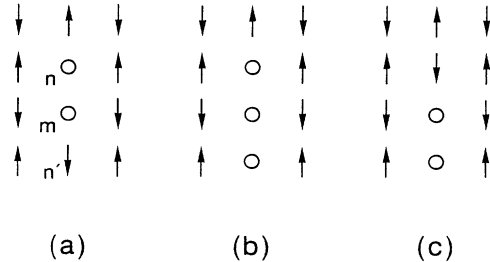


FIG. 2. A process that contributes to  $\langle n_{\mathbf{k},\downarrow} \rangle$ .

$$\delta \langle n_{\mathbf{k},\sigma} \rangle = \frac{c'}{N} \gamma(\mathbf{k}), \quad (21)$$

where the constant  $c'$  can be extracted from Tables I–IV. In Table V we now compare the numerical values for the momentum distribution obtained by summing up the different contributions from the string ansatz calculation with the data obtained in Ref. 9. One can see that the values are reasonably close, and especially the string picture is very capable of describing correctly the order of magnitude of the variation in  $\langle n_{\mathbf{k},\sigma} \rangle$ . Clearly the agreement is not particularly good. One should remember, however, that many approximations had to be made, especially concerning the two-hole ground-state wave function.

Since it seems impossible to distinguish between the different interpretations of the momentum distribution on the basis of its overall shape, one can consider its change under a change of hole doping or, equivalently, under a change of the system size for a fixed number of holes in the half-filled band. The string picture interpretation and the “band interpretation” would predict a quite different behavior of the momentum distribution: If one assumes that the shape of the momentum distribution is due to a band, which crosses the Fermi level, a change of the size of the cluster for fixed number of holes (which is equivalent to a change of the hole concentration) should lead to a change of  $\langle n_{\mathbf{k},\sigma} \rangle$  predominantly near the Fermi surface [see Fig. 3(a)]. On the other hand, the string picture would predict that one has an expression of the type  $\langle n_{\mathbf{k},\sigma} \rangle = \text{const} + \frac{1}{N} f(\mathbf{k})$ , i.e., under a change of  $N$  the  $\mathbf{k}$ -dependent part of  $\langle n_{\mathbf{k},\sigma} \rangle$  should scale with  $\frac{1}{N}$  throughout the Brillouin zone [see Fig. 3(b)]. One can conclude that the quantity

$$\eta_N = N(\langle n_{\mathbf{k}=(0,0),\sigma} \rangle - \langle n_{\mathbf{k}=(\pi,\pi),\sigma} \rangle) \quad (22)$$

should be independent of the cluster size  $N$  if the number of holes is kept fixed (e.g., two holes in a 20- or 18-site cluster). Indeed, by using the values given in Table I of Ref. 9 one finds  $\eta_{18} = 3.6736$  and  $\eta_{20} = 3.6868$  (these values are for  $J = 0.4$ ). While the number of lattice sites  $N$  changes by 10%, the quantity  $\eta_N$  changes by a mere 0.3%. Thus the change of  $\langle n_{\mathbf{k}} \rangle$  under the variation of the hole concentration is to very good approximation

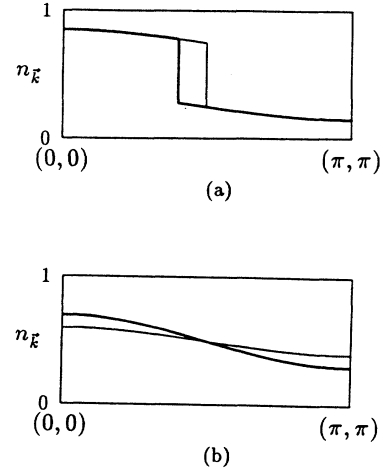


FIG. 3. Change of the momentum distribution function under a change of the hole concentration as expected from a band picture (a) and the string picture (b). The lower hole concentration corresponds to the thick line.

consistent with the predictions of the string picture. It should be noted that a more conclusive test would be possible using data from the 16-site cluster. Namely both the 16- and the 20-site cluster contain the point  $(\pi, 0)$  so that one could also check the  $N$  independence of the quantities

$$\eta'_N = N(\langle n_{\mathbf{k}=(0,0),\sigma} \rangle - \langle n_{\mathbf{k}=(\pi,0),\sigma} \rangle), \quad (23)$$

$$\eta''_N = N(\langle n_{\mathbf{k}=(\pi,\pi),\sigma} \rangle - \langle n_{\mathbf{k}=(\pi,0),\sigma} \rangle),$$

which would be particularly significant because  $(\pi, 0)$  is in the immediate neighborhood of the “large” Fermi surface.

To summarize this section it has been shown that the shape of the momentum distribution function as found in exact diagonalizations for the  $t$ - $J$  model is a general property of any system where the kinetic energy is given by a nearest-neighbor hopping term. Thus on the basis of this overall shape of the momentum distribution one cannot conclude that there is a corresponding Fermi

TABLE I. Contribution from different classes of processes depicted in Fig. 15 (the corresponding harmonic factors are listed in Table II).

$n^{(1)}$	$\frac{1}{2N} \left( \frac{1}{z-1} \beta_{0,0}^2 + \frac{z-2}{z-1} \sum_{\mu=0} \beta_{\mu,0}^2 \right) [2\gamma_{1,1}(\mathbf{k}) - \gamma_{2,0}(\mathbf{k})]$	Figs. 15(a) and 15(b)
$n^{(2)}$	$\frac{1}{N} (z-1)^{\frac{1}{2}} \sum_{\mu=0, \nu=0} \beta_{\mu,\nu} \beta_{\mu,\nu+1} \gamma(\mathbf{k})$	Fig. 15(c)
$n^{(3)}$	$\frac{1}{N} \frac{1}{(z-1)^{\frac{1}{2}}} \sum_{\mu=0, \nu=0} \beta_{\mu,\nu} \beta_{\nu+1,\mu} \gamma(\mathbf{k})$	Fig. 15(d)
$n^{(4)}$	$\frac{1}{N} \frac{1}{(z-1)^{\frac{1}{2}}} \sum_{\mu=0, \nu=0} \beta_{\mu,\nu+1} \beta_{\nu,\mu+2} \gamma(\mathbf{k})$	Fig. 15(e)
$n^{(5)}$	$\frac{1}{N} \frac{1}{(z-1)^{\frac{1}{2}}} \sum_{\mu=0, \nu=0} \beta_{\mu,\nu+1} \beta_{\mu+2,\nu} \gamma(\mathbf{k})$	Fig. 15(f)
$n^{(6)}$	$\frac{1}{N} \frac{1}{(z-1)^{\frac{1}{2}}} \sum_{\mu=0, \nu=0} \beta_{\mu,\nu+2} \beta_{\mu+3,\nu} \gamma(\mathbf{k})$	Fig. 15(g)

TABLE II. Harmonic factors used in different expressions.

$\gamma(\mathbf{k})$	$2[\cos(k_x) + \cos(k_y)]$
$\gamma_{1,1}(\mathbf{k})$	$2[\cos(k_x + k_y) + \cos(k_x - k_y)]$
$\gamma_{2,0}(\mathbf{k})$	$2[\cos(2k_x) + \cos(2k_y)]$

surface. This is all the more true because the ground state of two holes in a finite-cluster  $t$ - $J$  model is a bound state, where one cannot expect to obtain any kind of Fermi edge discontinuity at all. The numerical values of  $\langle n_{\mathbf{k},\sigma} \rangle$  over the whole Brillouin zone can be reproduced with reasonable accuracy using the string picture, which is also consistent with the numerical results of Poilblanc and Dagotto.<sup>29</sup> The doping dependence of  $\langle n_{\mathbf{k},\sigma} \rangle$ , as exemplified in the remarkable constancy of the quantity  $\eta_N$ , is in very good agreement with the string picture.

#### IV. SPECTRAL FUNCTION

Let us now turn to the discussion of the one-particle spectral function. First, let us consider the part corresponding to the creation of an additional hole in the ground state of the 18-site cluster  $t$ - $J$  model with two holes,  $|\Psi_0^{(2h)}\rangle$ . It can be written as

$$A_h(\mathbf{k}, \omega) = \sum_{\nu} |\langle \Psi_{\nu}^{(3h)} | c_{\mathbf{k},\uparrow} | \Psi_0^{(2h)} \rangle|^2 \delta(\omega - (E_{\nu}^{(3h)} - E_0^{(2h)})), \quad (24)$$

where  $E_0^{(2h)}$  is the ground-state energy of two holes and the sum over  $\nu$  runs over all eigenstates of three holes in the cluster.

As compared to the definition used in Ref. 9 we have omitted a constant shift in the argument of the  $\delta$  function but since we will be concerned predominantly with the dispersion of the peaks this is not of relevance. The rigid-band approximation would be well justified if the dispersion of the peaks with low excitation energy would be similar to that found for a single hole. Indeed Stephan and Horsch found, that “remnants” of the dispersion found for one single hole created in the Heisenberg antiferromagnet can be seen in the dispersion of the peak with the smallest excitation energy, i.e., the smallest  $|E_{\nu}^{(3h)} - E_0^{(2h)}|$ . In Fig. 4, the dispersion of the lowest

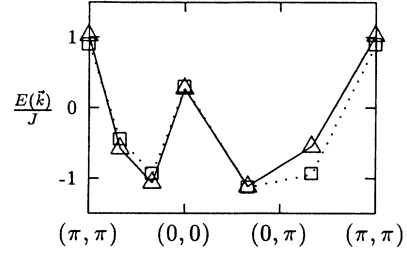


FIG. 4. Comparison of the  $\mathbf{k}$  dependence of the lowest excitation energy for the transition from two holes to three holes (squares) and from no holes to one hole (triangles) in an 18-site cluster. The ratio  $t/J = 2.5$ . The lines are guides to the eye.

energy peak obtained in the transition from two holes to three holes (extracted from Fig. 3(a) of Ref. 9) is compared with the respective dispersion obtained in the transition from no holes to one hole (extracted from Fig. 12 of Ref. 15, the dispersion for the transition from two to three holes is turned upside down as compared to Fig. 3 of Ref. 9). From this figure one can see that the two dispersions are essentially identical. Out of this band Stephan and Horsch have taken three peaks [the ones at  $(\frac{\pi}{3}, \frac{\pi}{3})$ ,  $(0, 0)$ , and  $(\frac{2\pi}{3}, 0)$ ] and interpreted them as part of a nearest-neighbor hopping band. Their main argument in doing so was the pole strength, which is particularly large for these peaks. It should be noted, however, that even for a single hole the pole strength along the (next-nearest-neighbor) quasiparticle band has a rather pronounced  $\mathbf{k}$  dependence, which can be explained very well by the string picture.<sup>21</sup> Especially, the pole strength is significantly smaller outside the magnetic Brillouin zone (i.e., the Fermi surface of the free half-filled band) than inside (see, e.g., Fig. 6 in Ref. 21). Thus the  $\mathbf{k}$  dependence of the pole strength found by Stephan and Horsch is not a new feature of the doped case, but is qualitatively the same as for the single hole.

Let us now turn to the spectral function describing the creation of an electron. This can be written as

$$A_e(\mathbf{k}, \omega) = \sum_{\mu} |\langle \Psi_{\mu}^{(1h)} | c_{\mathbf{k},\uparrow}^{\dagger} | \Psi_0^{(2h)} \rangle|^2 \delta(\omega - (E_{\mu}^{(1h)} - E_0^{(2h)})), \quad (25)$$

TABLE III. Contribution from different classes of processes depicted in Fig. 16.

$n^{(7)}$	$-\frac{2}{N} \frac{1}{z-1} \sum_{\mu=0} \beta_{\mu,1} \beta_{0,\mu+1} \gamma_{2,0}(\mathbf{k})$	Fig. 16(a)
$n^{(8)}$	$-\frac{1}{N} \frac{1}{(z-1)} \sum_{\mu=0, \nu=1} \beta_{\mu,\nu}^2 [\gamma_{2,0}(\mathbf{k}) + 2\gamma_{1,1}(\mathbf{k})]$	Fig. 16(b)
$n^{(9)}$	$-2 \frac{1}{N} \frac{1}{(z-1)^2} \sum_{\mu=2} \beta_{\mu,0} \beta_{2,\mu-2} \gamma_{2,0}(\mathbf{k})$	Fig. 16(c)
$n^{(10)}$	$\frac{1}{N} \frac{1}{(z-1)^2} \left( \frac{1}{z-1} \beta_{2,0}^2 + \frac{z-2}{z-1} \sum_{\mu=2} \beta_{\mu,0}^2 \right) \gamma_{1,1}(\mathbf{k})$	Fig. 16(d)
$n^{(11)}$	$2 \frac{1}{N} \frac{1}{(z-1)^2} \left( \frac{1}{z-1} \beta_{2,0}^2 + \frac{z-2}{z-1} \sum_{\mu=2} \beta_{\mu,0} \beta_{\mu-2,2} \right) \gamma_{1,1}(\mathbf{k})$	Fig. 16(e)
$n^{(12)}$	$\frac{1}{N} \frac{1}{(z-1)^2} \left( \frac{1}{z-1} \beta_{2,0}^2 + \frac{z-2}{z-1} \sum_{\mu=0} \beta_{\mu,2}^2 \right) \gamma_{1,1}(\mathbf{k})$	Fig. 16(f)

TABLE IV. Contribution from different classes of processes depicted in Fig. 17.

$n^{(13)}$	$-\frac{2}{N} \frac{1}{(z-1)^2} \left( \frac{1}{z-1} \sum_{\mu=0} \beta_{\mu,2} \beta_{1,\mu+1} + \frac{z-2}{z-1} \sum_{\mu=0,\nu=2} \beta_{\mu,\nu} \beta_{\nu-1,\mu+1} \right)$ $\left[ \gamma_{2,0}(\mathbf{k}) + 2\gamma_{1,1}(\mathbf{k}) \right]$	Fig. 17(a)
$n^{(14)}$	$\frac{2}{N} \frac{1}{(z-1)^2} \left( \frac{1}{z-1} \beta_{2,0} \beta_{1,1} + \frac{z-2}{z-1} \sum_{\mu=2} \beta_{\mu,0} \beta_{1,\mu-1} \right) \gamma_{1,1}(\mathbf{k})$	Fig. 17(b)
$n^{(15)}$	$\frac{2}{N} \frac{1}{(z-1)^2} \left( \frac{1}{z-1} \beta_{2,0} \beta_{1,1} + \frac{z-2}{z-1} \sum_{\mu=0} \beta_{2,\mu} \beta_{\mu+1,1} \right) \gamma_{1,1}(\mathbf{k})$	Fig. 17(c)
$n^{(16)}$	$\frac{1}{N} \frac{1}{(z-1)^2} \left( \frac{1}{z-1} \beta_{1,1}^2 + \frac{z-2}{z-1} \sum_{\mu=1} \beta_{\mu,1}^2 \right) \gamma_{1,1}(\mathbf{k})$	Fig. 17(d)

where the sum over  $\mu$  runs over all eigenstates with one hole. Here the numerical data<sup>9</sup> at first sight show a clear contradiction with what one may expect from the rigid-band approximation: one would guess that a sizable spectral intensity can be seen only near the the ground-state momentum of one hole,  $\mathbf{k}_0 = (\frac{2\pi}{3}, 0)$ . The spectra shown in Ref. 9, however, show sizable intensity for quite a number of  $\mathbf{k}$  points. On the other hand, one again has to bear in mind the fact that the ground state of two holes in a finite cluster is a bound state. To see the consequences, let us again consider the simple wave function (12). By annihilating one “quasiparticle” in this state one obtains

$$a_{\mathbf{k},\uparrow} |\Psi_0\rangle = \Delta(\mathbf{k}) a_{-\mathbf{k},\downarrow}^\dagger |0\rangle. \quad (26)$$

This has two consequences: First, there is a nonvanishing pole strength whenever the “bound-state wave function”  $\Delta(\mathbf{k})$  is different from zero for the respective  $\mathbf{k}$  point. In other words, one may not expect to find a line in  $\mathbf{k}$  space where the pole strength  $Z_h$  discontinuously drops to zero. Second, the spectral weight  $Z_h$  will be proportional to  $|\Delta(\mathbf{k})|^2$ , which is determined entirely by the internal structure of the bound state and which may very well have a sizable influence on its  $\mathbf{k}$  dependence. In fact, as has been mentioned in the discussion of the momentum distribution function, the interaction of the holes may be expected to lead to an appreciable redistribution of the holes in  $\mathbf{k}$  space. In addition, as will be shown below, the special symmetry of the two-hole ground-state wave function and the resulting selection rules completely dominate the  $\mathbf{k}$  dependence of the pole strength in the spectral function  $A_e(\mathbf{k}, \omega)$ .

To be more specific, let us first note that by creating a hole in the ground state  $|\Psi_0^{(0h)}\rangle$  of the Heisenberg antiferromagnet and by annihilating a hole in the two-hole ground state  $|\Psi_0^{(2h)}\rangle$  one is probing the same manifold of final states  $|\Psi_\nu^{(1h)}(\mathbf{k})\rangle$  (both  $|\Psi_0^{(0h)}\rangle$  and  $|\Psi_0^{(2h)}\rangle$  are spin singlets and have zero momentum). The only difference is in the pole strengths, which are given by

$$|\langle \Psi_\nu^{(1h)}(\mathbf{k}) | c_{\mathbf{k},\uparrow}^\dagger | \Psi_0^{(2h)} \rangle|^2 \quad (27)$$

and

$$|\langle \Psi_\nu^{(1h)}(\mathbf{k}) | c_{-\mathbf{k},\downarrow} | \Psi_0^{(0h)} \rangle|^2. \quad (28)$$

For  $J = 0.4t$ , the peak with the lowest excitation energy  $|E_\mu^{(1h)} - E_0^{(2h)}|$  in the inverse photoemission spectrum in Ref. 9 is situated at  $\mathbf{k} = (\frac{2\pi}{3}, 0)$ , the ground-state momentum of a single hole in the 18-site cluster  $t$ - $J$  model for this value of  $t/J$ . Thus it seems reasonable to assume that the state responsible for this peak is indeed the single-hole ground state. Then, in Fig. 5 the dispersion of the lowest excitation energy for the transition from two holes to one hole (extracted from Fig. 3(a) of Ref. 9) and the transition from no holes to one hole (extracted from Fig. 12 of Ref. 15) are compared under the assumption, that the peaks at  $(\frac{2\pi}{3}, 0)$  in both spectral functions originate from the same final state, i.e., the ground state of the cluster with one hole. One can see that at  $(\frac{2\pi}{3}, 0)$  as well as at  $(\pi, \frac{\pi}{3})$  there appear to be observable transitions from the two-hole ground state into the “quasiparticle band.” [Thereby it is unclear why for momentum  $(\pi, \frac{\pi}{3})$  the peak obtained in the transition

TABLE V. Momentum distribution for the  $4 \times 4$  and 18-site cluster in the two-hole ground state. The table shows the exact diagonalization data of Stephan and Horsch (Ref. 9) (SH) and the results of the string calculation (string).

$\mathbf{k}$	$n_{\mathbf{k},\sigma}$ (SH)	$n_{\mathbf{k},\sigma}$ (string)	$\mathbf{k}$	$n_{\mathbf{k},\sigma}$ (SH)	$n_{\mathbf{k},\sigma}$ (string)
(0, 0)	0.54681	0.53671	(0, 0)	0.55160	0.54078
$(\frac{2\pi}{5}, \frac{\pi}{5})$	0.54016	0.53870	$(\frac{\pi}{3}, \frac{\pi}{3})$	0.55111	0.54396
$(\frac{\pi}{5}, \frac{3\pi}{5})$	0.51224	0.50475	$(\frac{2\pi}{3}, 0)$	0.50406	0.49069
$(\pi, 0)$	0.47270	0.43703	$(\frac{2\pi}{3}, \frac{2\pi}{3})$	0.35993	0.37411
$(\frac{4\pi}{5}, \frac{2\pi}{5})$	0.37804	0.42832	$(\pi, \frac{\pi}{3})$	0.36012	0.40577
$(\frac{3\pi}{5}, \frac{4\pi}{5})$	0.35589	0.36779	$(\pi, \pi)$	0.34751	0.20110
$(\pi, \pi)$	0.36247	0.23100			

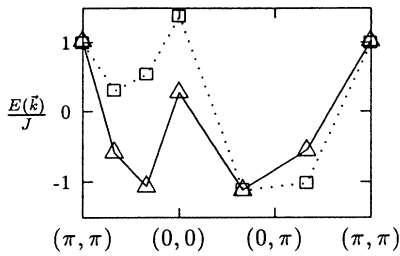


FIG. 5. Comparison of the  $\mathbf{k}$  dependence of the lowest excitation energy for the transition from two holes to one hole (squares) and from no holes to one hole (triangles) in an 18-site cluster. The ratio  $t/J = 2.5$ . The lines are guides to the eye.

from two holes to three holes is lower in energy than the one obtained in the transition from no holes to one hole.] On the other hand, along  $(0, 0)$ - $(\pi, \pi)$  there appear to be no transitions to the quasiparticle band. Rather the peaks obtained by starting from the two-hole ground state are an energy of at least  $J$  above this band. This is readily traced back to a symmetry-related selection rule: For any  $\mathbf{k}$  point along the  $(1, 1)$  direction the operation  $T_m$  which consists of reflection by a plane along  $(1, 1)$  and perpendicular to the basal plane belongs to the little group of that  $\mathbf{k}$  point. Now there is overwhelming numerical evidence<sup>26,22,24,28</sup> that the ground state of two holes,  $|\Psi_0^{(2h)}\rangle$ , has  $d_{x^2-y^2}$  symmetry in other words: it is odd under  $T_m$ . On the other hand, it seems obvious that the ground state of the Heisenberg antiferromagnet,  $|\Psi_0^{(0h)}\rangle$ , has the full symmetry of the lattice. In other words, it is even under  $T_m$ . Thus, by inspection of the expressions for the matrix elements (27) and (28) one can deduce that any state  $|\Psi_\nu(\mathbf{k})\rangle$ , which can be observed by creating a hole with momentum in  $(1, 1)$  direction in the ground state of the Heisenberg antiferromagnet (HAF), cannot be observed by creating an electron in the two-hole ground state and vice versa. This explains why the poles in the spectral function  $A_e(\mathbf{k}, \omega)$  along the  $(1, 1)$  direction are much higher than the ones in the spectral function for the creation of a hole at half filling.

More evidence for this interpretation is provided by the work of Hasegawa and Poilblanc.<sup>22</sup> These authors have evaluated the lowest-energy states for all possible momenta and for all irreducible representations of the corresponding little groups in 16- and 18-site clusters of the  $t$ - $J$  model. In Fig. 6 the energy dispersions of the lowest one-hole states with total spin  $s = \frac{1}{2}$  for representations, which are even ( $A_1$  representation) and odd [this is the  $A_2$  representation for all points along  $(1, 1)$  except for  $(0, 0)$  and  $(\pi, \pi)$ , for which it is the  $B_1$  representation] under  $T_m$ , are compared to the data from Ref. 9. Thereby the relative location of the energies obtained by Hasegawa and Poilblanc for the 16- and 18-site clusters was fixed by identifying the energies of the  $A_1$  states at momentum  $(0, 0)$ . The relative location of the energies between the data of Stephan and Horsch, and Hasegawa and Poilblanc was done by identifying the ground-state

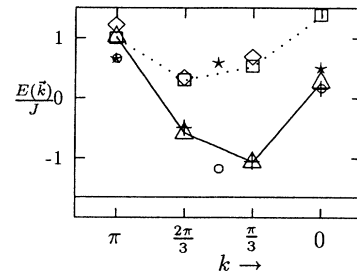


FIG. 6. Dispersion of the lowest excitation energies as obtained in Ref. 9 in the transition from two holes to one hole (squares) and in Ref. 15 for the transition from no holes to one hole (triangles) for  $\mathbf{k} = (k, k)$ . These are compared to the energies of states transforming according to the  $A_1$  representation in the 18-site cluster (crosses) and the 16-site cluster (circles) as well as states transforming according to the  $A_2$  or  $B_1$  representation in the 18-site cluster (diamonds) and the 16-site cluster (stars) as obtained by Hasegawa and Poilblanc (Ref. 22). The full line corresponds to the Fermi energy introduced in Ref. 9.

energies. In the data of Hasegawa and Poilblanc one can roughly identify two “bands,” one of them consisting of crosses and circles (these are the states belonging to the trivial representation  $A_1$ ) and the other one consisting of diamonds and stars (these are states belonging to the representations  $A_2$  and  $B_1$ , which are odd under  $T_m$ ). The stars at  $(0, 0)$  and  $(\pi, \pi)$  do not fit very well into this band, but it should be noted that the  $4 \times 4$  cluster from which they are obtained has many additional degeneracies which are absent in the 18-site cluster. In addition arguments will be presented below that the higher-lying  $A_2$  states are more susceptible to finite-size effects. Obviously, the states observed by Stephan and Horsch in the inverse photoemission spectrum (squares) are all lying in the “ $A_2$  band,” and they are indeed remarkably close to the states found by Hasegawa and Poilblanc in the 18-site cluster (diamonds) (this is all the more remarkable because the spectrum in Ref. 9 has been evaluated for  $t/J = 2.5$  whereas the calculation of Hasegawa and Poilblanc has been performed for  $t/J = 4$ ; when measured in units of  $J$ , however, the dispersion relation for the individual bands seems to have little dependence on the ratio  $t/J$ ). This shows that the above symmetry arguments indeed determine the inverse photoemission spectrum. However, one can also see something else if one takes into account the additional information provided by the data of Hasegawa and Poilblanc from the 16-site cluster (circles and stars): one can clearly see that there is not a single state having the correct symmetry to be observed in inverse photoemission starting from the two-hole ground state, which is closer than  $\sim 2J$  to the “Fermi level” introduced in Ref. 9 (shown as the full line in Fig. 6). Thus an interpretation of the spectra in terms of a band that approaches and even crosses this Fermi level seems highly questionable. Using the results of Hasegawa and Poilblanc shown in Fig. 6 and the selec-

tion rule explained above, one can predict that the lowest state which can be reached with a nonvanishing matrix element by creating an electron with momentum  $(\frac{\pi}{2}, \frac{\pi}{2})$  in the ground state of two holes in the  $4 \times 4$  cluster [the star at  $(\frac{\pi}{2}, \frac{\pi}{2})$ ] would lie almost an energy of  $2J$  above the large Fermi surface whereas it should be immediately above it if the interpretation in terms of a nearest neighbor hopping band were correct. This provides quite a strong argument against the large Fermi surface, because a quasiparticle band should be particularly well defined in the neighborhood of the Fermi surface, whereas in inverse photoemission along the  $(1, 1)$  direction there will be no observable state that is closer to the Fermi energy than  $\sim 2J$ , i.e., almost half of the width of the proposed nearest-neighbor hopping band.

Let us now briefly summarize what we believe is the correct interpretation of the spectra shown in Fig. 3 of Ref. 9 (see Fig. 7): in the  $\omega < 0$  part of the spectral function one obtains again the quasiparticle band found already in the transition from no holes to one hole.<sup>15</sup> This interpretation is suggested by the very good agreement of the dispersion curves obtained in the transition from no to one hole and from two to three holes (see Fig. 4), which seems too good to be mere coincidence.

In the  $\omega > 0$  part of the spectral function at  $(\frac{2\pi}{3}, 0)$  and at  $(\frac{\pi}{3}, \pi)$  one has transitions into the familiar quasiparticle band for one hole. This is suggested by the fact, that the ground state of a single hole (which belongs to this quasiparticle band) is known to be at  $(\frac{2\pi}{3}, 0)$  and the peak with the lowest excitation energy in the inverse photoemission spectrum is indeed at this momentum (for  $t/J = 2.5$ ). Along the  $(1, 1)$  direction a selection rule forbids transitions into the quasiparticle band and the lowest states, that can be reached with a nonvanishing matrix element belong to a higher-lying, symmetry-different band. This interpretation is confirmed by comparison with the data of Hasegawa and Poilblanc<sup>22</sup>.

While nothing can be said about what the inverse photoemission spectrum would look like if one did not start from a bound state with special symmetry, one can see that in the spectral function for the creation of an additional hole there is again the same next-nearest-neighbor hopping dispersion with a bandwidth of  $2J$  which was

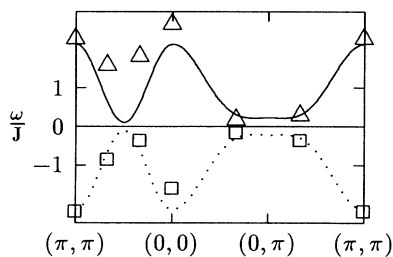


FIG. 7. This figure summarizes our interpretation of the spectral functions  $A_h(\mathbf{k}, \omega)$  (this is the negative frequency part of the figure, i.e., squares) and  $A_e(\mathbf{k}, \omega)$  (positive frequency part, triangles) as obtained in Ref. 9. The figure directly can be compared to Fig. 3(a) of that reference.

already observed in the creation of a single hole in the ground state of the HAF. This is precisely what one would expect from the rigid-band approximation, and therefore it seems that this approximation is very well justified until well into the range of dopings where superconductivity occurs. Thus what remains to be done is to explain the higher-lying  $A_2$  band along the  $(1, 1)$  direction as well as the  $\mathbf{k}$  dependence of the matrix elements for transitions into this band in the framework of the string picture. Here the following should be stressed: this band has never been observed in any numerical study of the one-hole spectral function in the  $t$ - $J$  model. This, however, is prevented by the above-mentioned selection rule and therefore by no means excludes the existence of such a band.

## V. STRING CALCULATIONS

First, we consider the possible final states  $|\Psi_\nu(\mathbf{k})\rangle$  for inverse photoemission when  $\mathbf{k}$  is along the  $(1, 1)$  direction. From the above analysis one can conclude, that in order to be observable, these states have to be odd under  $T_m$  or, stated differently, they should transform according to the  $A_2$  representation of the little group of  $\mathbf{k}$  points along the  $(1, 1)$  direction. For the description of the  $T_m$  even (or  $A_1$ ) quasiparticle band we have chosen [see Eq. (5)] a coherent superposition of localized states, which in turn are linear combinations of individual string states. Thus the quasiparticle has an internal structure and this internal structure will also contribute to the transformation properties of the wave function. In order to obtain a wave function belonging to the  $A_2$  representation it is sufficient to choose a coherent superposition of states  $|\tilde{\Phi}_j\rangle$ , which are odd under  $T_m$ , i.e., which satisfy  $T_m|\tilde{\Phi}_j\rangle = -|\tilde{\Phi}_j\rangle$  (thereby it is assumed that the mirror plane goes through the central site  $j$ ). There are actually two different types of states which have this property: a state with  $d_{x^2-y^2}$ -type symmetry and a state with  $p_{x-y}$ -type symmetry. These can be written as

$$|\tilde{\Phi}_j^{(1)}\rangle = \sum_{\nu=1}^{\infty} \tilde{\alpha}_\nu^{(1)} \sum_{\mathcal{P}} \phi_1(\mathcal{P}) |j, \nu, \mathcal{P}\rangle, \quad (29)$$

$$|\tilde{\Phi}_j^{(2)}\rangle = \sum_{\nu=1}^{\infty} \tilde{\alpha}_\nu^{(2)} \sum_{\mathcal{P}} \phi_2(\mathcal{P}) |j, \nu, \mathcal{P}\rangle.$$

Thereby the extra factors  $\phi_1(\mathcal{P}), \phi_2(\mathcal{P})$  are determined by the direction of the first step of the path  $\mathcal{P}$  as indicated in Fig. 8. This choice of the phase factors makes sure that the states defined above have the correct transformation properties. As in the case of the symmetric quasiparticle, the coefficients  $\tilde{\alpha}_\nu^{(\mu)}$ , which are assumed to depend only on the length of the path, are determined from the requirement that these states are eigenstates of  $H_0$  in the subspace of string states with starting point  $j$ . Inserting them into the Schrödinger equation and introducing  $\tilde{\beta}_\nu^{(\mu)} = \tilde{\alpha}_\nu^{(\mu)} / (z-1)^{\frac{z}{2}}$  one finds that the  $\tilde{\beta}_\nu^{(\mu)}$  both have to obey the same set of difference equations:

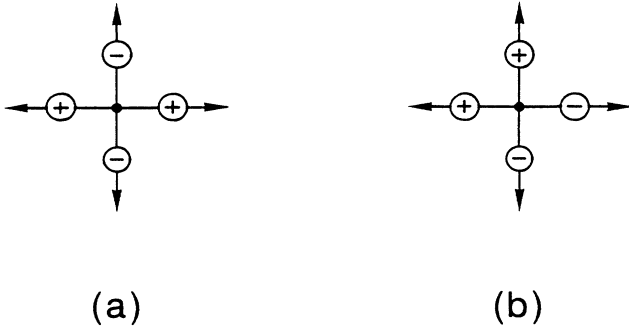


FIG. 8. Dependence of the phase factors  $\phi_1(\mathcal{P})$  (a) and  $\phi_2(\mathcal{P})$  (b) on the direction of the first hop along the path  $\mathcal{P}$ .

$$-\tilde{t}(\tilde{\beta}_{\nu+1} + \tilde{\beta}_{\nu-1}) + (\nu + \frac{1}{2})J\tilde{\beta}_\nu = \tilde{E}_B\tilde{\beta}_\nu, \quad (30)$$

where it is understood that  $\tilde{\beta}_0 = 0$  and the superscript  $\mu$  will be omitted henceforth. These equations are the analog of (4) for the symmetric quasiparticle, and  $\tilde{E}_B$  is the binding energy of the localized state. The difference  $\tilde{E}_B - E_B$  [where  $E_B$  is defined in (4)] then determines essentially the separation in energy between the original ( $A_1$ ) quasiparticle band and the  $A_2$  band. This quantity is shown in Fig. 9 as a function of  $t/J$ , and it is indeed a constant of order  $1.5J$ . This can be understood by inspection of the two sets of equation systems, (4) and (30). Since one has  $\tilde{\beta}_0 = 0$ , the minimum length of the string in the  $A_2$  wave function is 1, and therefore the smallest value of the “string potential” is  $1.5J$  (the first step creates three frustrated bonds), whereas it is zero for the symmetric state. It should be noted that Fig. 9 is essentially the explanation why the “bandwidth” in the  $\omega > 0$  part in Fig. 3 of Ref. 9 scales with  $J$ : this bandwidth is mostly due to the separation between the  $A_1$  states and the  $A_2$  states.

This observation also allows for another cross check against exact diagonalizations: both the Schrödinger equations for the symmetric and antisymmetric quasiparticles have a linearly ascending potential with the same slope. If one replaces  $\frac{z}{z-1} \rightarrow 1$  in Eq. (4) and ignores the fact that in this equation in the first step the string potential increases by  $1.5J$  rather than  $J$ , these equations are actually identical, except for a shift in the index  $\nu$  and

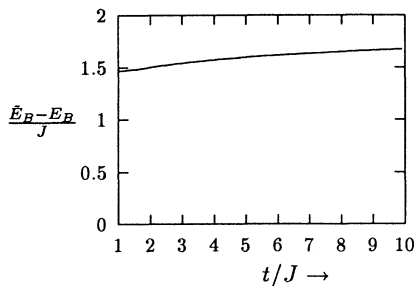


FIG. 9. Energy difference  $(\tilde{E}_B - E_B)/J$  as a function of the ratio  $t/J$ .

a constant shift of the string potential by  $1.5J$ . Consequently one could expect that the solutions are quite similar except for a shift in the index  $\nu$ :  $\tilde{\beta}_\nu \simeq \beta_{\nu-1}$ . Hence the expectation values of the kinetic energy, which can be written as

$$\langle H_t \rangle = -tz[\alpha_0\alpha_1 + (z-1)\alpha_1\alpha_2 + \dots], \quad (31)$$

$$\langle H_t \rangle' = -tz(z-1)[\tilde{\alpha}_1\tilde{\alpha}_2 + (z-1)\tilde{\alpha}_2\tilde{\alpha}_3 + \dots],$$

should be essentially identical for the lowest ( $A_1$ ) states and the  $A_2$  (or  $B_1$ ) states along the  $(1,1)$  direction and it should be so independently of the momentum. By inspection of Tables II and III of the paper by Hasegawa and Poilblanc<sup>22</sup> one can see that the expectation value of the kinetic energy indeed shows a significantly smaller variation both under a change of the momentum and under a change of the irreducible representation than the total energy. This is precisely what one would expect from the string picture interpretation and we believe that this provides good evidence for our interpretation of these states.

Next, for a state with momentum  $\mathbf{k}$  we make the ansatz

$$|\tilde{\Psi}(\mathbf{k})\rangle = \sum_{\mu=1}^2 c_\mu |\tilde{\Psi}^{(\mu)}(\mathbf{k})\rangle, \quad (32)$$

$$|\tilde{\Psi}^{(\mu)}(\mathbf{k})\rangle = \sqrt{\frac{2}{N}} \sum_j e^{-i\mathbf{k}\cdot\mathbf{R}_j} |\tilde{\Phi}_j^{(\mu)}\rangle.$$

It should be noted that along the  $(1,1)$  direction this ansatz is particularly suited because from group theory one knows, that there can be only states which are either odd or even under  $T_m$ . The coefficients  $c_{1,2}$  are variational parameters and to set up the variational equations one can proceed in a completely analogous fashion as in Ref. 14 for the symmetric quasiparticles. Then it can be shown (Appendix A) that to good approximation one obtains two dispersionless bands with energies

$$E_{1,2}(\mathbf{k}) = E_{\text{Néel}} + J + \tilde{E}_B + 4\tilde{h}_1 + 2\tilde{h}_2 \pm 2\tilde{h}_2, \quad (33)$$

$$\tilde{h}_1 = \frac{J}{(z-1)^2} \sum_{\nu=1}^{\infty} \tilde{\beta}_\nu \tilde{\beta}_{\nu+2},$$

$$\tilde{h}_2 = \frac{2\tilde{t}}{(z-1)^3} \tilde{\beta}_2 \tilde{\beta}_3,$$

and the respective eigenvectors are

$$|c_1|^2 = \frac{1}{2}[1 \pm \cos(2k)], \quad (34)$$

$$|c_2|^2 = \frac{1}{2}[1 \mp \cos(2k)].$$

The dispersion relations for the  $A_1$  band and the  $A_2$  bands are shown in Fig. 10 and are compared to the results of Hasegawa and Poilblanc. One can see that particularly for the  $A_2$  bands there is not a very good agreement. It should be noted, however, that the functions  $|\tilde{\Phi}_j^{(\mu)}\rangle$  are much more delocalized than the function

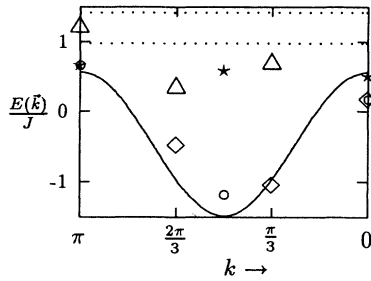


FIG. 10. Dispersion of  $A_1$  band (full line) and the  $A_2$  bands (dashed lines) as obtained from the string ansatz along the  $(1,1)$  direction. The diamonds (circles) correspond to the  $A_1$  states of Hasegawa and Poilblanc for the 18 (16) site cluster, the triangles (stars) to the  $A_2$  states. The ratio  $J/t = 0.25$ .

$|\Phi_j\rangle$  (they have a node in the center), so they are certainly much more sensible to the finite size of the cluster. Thus one can expect much stronger finite-size effects for these bands. On the other hand, the range of energies where the  $A_2$  bands should be situated is predicted reasonably well by the string ansatz.

Next, let us proceed to the  $\mathbf{k}$  dependence of the pole strength for transitions from the two-hole ground state  $|\Psi_0^{(2h)}\rangle$  into the  $A_2$  bands. To that end, we use again the wave function (16) used already in the calculation of the momentum distribution function. We then need to know the matrix elements

$$m_\mu(\mathbf{k}) = \langle \tilde{\Psi}^{(\mu)}(\mathbf{k}) | c_{\mathbf{k},\sigma}^\dagger | \Psi_d \rangle, \quad (35)$$

which can be written as

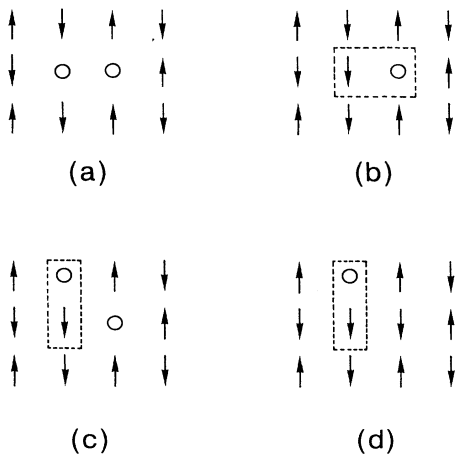


FIG. 11. Some processes that give rise to a nonvanishing contribution to  $\langle \tilde{\Psi}_j | c_{l,\uparrow}^\dagger | \Phi_{m,n} \rangle$ . The state shown in (a), which is a “double string” of length 0 is thereby transformed into a string of length 1, shown in (b). The state shown in (c), which is a “double string” of length 1 is transformed into a string of length 1, shown in (d).

$$m_\mu(\mathbf{k}) = \frac{1}{\sqrt{2N^3}} \sum_{m \in A, n, l} e^{i\mathbf{k} \cdot (\mathbf{R}_j - \mathbf{R}_l)} \epsilon_{m,n} \langle \tilde{\Phi}_j^{(\mu)} | \hat{c}_{l,\uparrow}^\dagger | \Phi_{m,n} \rangle. \quad (36)$$

Let us first consider the matrix element of the type  $\langle \tilde{\Phi}_j^{(1)} | \hat{c}_{l,\uparrow}^\dagger | \Phi_{m,n} \rangle$ . There are various processes which give rise to nonvanishing matrix elements of this type. Examples are shown in Fig. 11. From the state shown in 11(a) the one in 11(b) can be obtained by creation of an electron. This is a string of length 1, which has expansion coefficient  $\tilde{\alpha}_1$ . There is an additional minus sign from fermion anticommutation relations so that one obtains a contribution of  $-\alpha_{0,0}\tilde{\alpha}_1$ . In this process one has to identify  $j = l = m$ , so the phase factor is unity.

From the state shown in Fig. 11(c) the one in 11(d) is obtained. This is a string of length 1 in the  $y$  direction, and in the state  $|\tilde{\Phi}_j^{(1)}\rangle$  it has the expansion coefficient  $-\tilde{\alpha}_1$ . In this process one should identify  $j = m$  and  $l = n$  so the phase factor associated with this contribution is  $e^{-ik_x}$ . There is again an extra minus sign due to fermion anticommutation relations, so that the total contribution to  $m_1$  is  $\alpha_{0,1}\tilde{\alpha}_1 e^{ik_x}$ . Collecting all possible processes involving strings of length  $l < 4$  one arrives after some straightforward calculations at the following expressions for the matrix elements:

$$\begin{aligned} m_1(\mathbf{k}) &= \frac{1}{\sqrt{N}} \{x_1 + x_2[\cos(k_x) + \cos(k_y)]\}, \\ x_1 &= -(2\alpha_{0,0}\tilde{\alpha}_1 + 8\alpha_{0,1}\tilde{\alpha}_2 + 20\alpha_{0,2}\tilde{\alpha}_3 + 6\alpha_{1,1}\tilde{\alpha}_3), \\ x_2 &= (4\alpha_{0,1}\tilde{\alpha}_1 + 6\alpha_{0,2}\tilde{\alpha}_2 + 9\alpha_{1,1}\tilde{\alpha}_2), \\ m_2(\mathbf{k}) &= ix_3[\sin(k_x) + \sin(k_y)], \\ x_3 &= (4\alpha_{0,2}\tilde{\alpha}_2 + 6\alpha_{1,1}\tilde{\alpha}_2). \end{aligned} \quad (37)$$

It should be noted that the general form of this expression is determined essentially by the symmetry of the string states and the geometry of the individual strings. Thus, while the coefficients  $x_{1,2,3}$  might change slightly if longer strings are taken into account, there will be no change in the overall form. The overall form of  $m_1(\mathbf{k})$  leads already to a  $\mathbf{k}$  dependence of the pole strength for transitions into the  $A_2$  bands which is qualitatively the same as observed by Stephan and Horsch:<sup>9</sup> it is large near the corner of the zone and small near the center. This behavior is then still modulated by the eigenvectors  $(c_1, c_2)$ . The resulting pole strengths for transitions from the two-hole ground state into the two  $A_2$  bands is shown in Fig. 12 as a function of the wave vector  $\mathbf{k}$ . Obviously, the overall trend in the exact diagonalizations comes out correctly: the residuum is very small in the center of the Brillouin zone, but large near the corner. It is hard to uniquely assign the exact diagonalization points to the bands, but it should be noted that the information from the finite clusters is not sufficient to do this: for some representations (such as the two-dimensional  $E$  representation) Hasegawa and Poilblanc did not give the energy of the state with total spin  $s = \frac{1}{2}$ . At the highly symmetric points  $(0,0)$  and  $(\pi,\pi)$ , however, the  $A_2$  band must be connected smoothly to states which transform according to the  $B_1$  and  $E$  representations (this comes out in the string calculations as can be verified by inspection of the

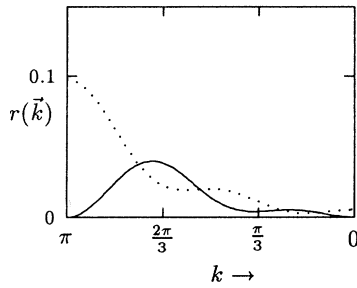


FIG. 12. Pole strengths for the creation of an electron with momentum  $(k, k)$  in the two-hole ground state as obtained from the string ansatz along the  $(1, 1)$  direction. The dashed line corresponds to the lower  $A_2$  band, the dashed dotted line to the higher one. The ratio  $J/t = 0.4$ .

eigenvectors).

Another point is that in the exact diagonalizations the pole strength at  $\mathbf{k} = (\frac{2\pi}{3}, \frac{2\pi}{3})$  is larger than at  $\mathbf{k} = (\pi, \pi)$  in contrast to the analytical result. It should be borne in mind, however, that the analytical calculation certainly is very rough because many strong approximations (especially concerning the ground-state wave function  $|\Psi_0^{(2h)}\rangle$ ) had to be made. However, it seems fair to say that both the range of energies where the  $A_2$  bands should lie as well as the  $\mathbf{k}$  dependence of the pole strength  $\tilde{r}(\mathbf{k})$  describing transitions from the two-hole ground state into this band can be predicted roughly correctly by the string picture. From that point of view all the data in Ref. 9 are at least qualitatively in agreement with the string picture.

## VI. CONCLUSION

In the preceding sections it has been shown that the exact diagonalization results<sup>9</sup> for the momentum distribution and one-particle spectral function in the two-hole ground state of finite-cluster  $t$ - $J$  models can be reproduced at least qualitatively by the string picture.

In Ref. 9 it was concluded that the single-hole case is “a problem of only marginal relevance” for the moderately doped case and that possible theories of the  $t$ - $J$  model have to reproduce a large Fermi surface and a nearest-neighbor hopping band. In this interpretation, the ground state of two holes is viewed as a representative for a Fermi sea of quasiparticles.

We find on the contrary, that the two-hole case can be treated as the natural extension of the single-hole case and that there is neither a large Fermi surface nor a nearest-neighbor hopping band. In our interpretation, the two-hole ground state is simply a bound state of two spin bags and does not represent an infinite system at finite doping.

We would like to summarize the arguments which we believe to be in favor of our interpretation.

(a) It is easy to see that the shape of the momentum-distribution function found in exact diagonalizations is a general property of any system where the kinetic energy is given by a nearest-neighbor hopping term. Thus on the basis of this shape of  $\langle n_{\mathbf{k},\sigma} \rangle$  found on a finite  $\mathbf{k}$  mesh

one cannot conclude that there is a correspondingly large Fermi surface and therefore one of the key arguments in favor of the large Fermi surface is invalid.

(b) Our interpretation takes into account the fact that the two-hole ground state is a bound state with nontrivial symmetry. This is important, first because it excludes any kind of discontinuity both in the momentum distribution and the quasiparticle pole strength, second because it gives a contribution to  $\langle n_{\mathbf{k},\sigma} \rangle$ , which is determined by the “internal structure” of the bound state, and third because it enforces selection rules in the spectral function.

(c) Our interpretation reconciles the apparently contradicting results of Stephan and Horsch<sup>9</sup> and of Poilblanc and Dagotto<sup>29</sup> in a simple way.

(d) The change in the momentum-distribution function under a change of the hole concentration is to very good accuracy consistent with our explanation in terms of the string picture.

(e) Our interpretation of the low-lying peaks in the spectral function for the creation of an electron is confirmed by the data of Hasegawa and Poilblanc.<sup>22</sup> In addition, by making use of these data one can predict that in the  $4 \times 4$  cluster the peak in the spectral function for the creation of an electron at  $(\frac{\pi}{2}, \frac{\pi}{2})$  (which is particularly significant because it is very close to the “large Fermi surface”) must be an energy of  $\sim 2J$  away from the nearest-neighbor hopping band and the corresponding “large Fermi surface” introduced in Ref. 9, making this band a highly implausible interpretation.

(f) Our interpretation is consistent with the work of Dagotto and Schrieffer.<sup>28</sup> These authors have first constructed “quasiparticle operators,” which describe the wave function for a single hole in a finite cluster very well. In a second step they constructed a two-hole wave function with the correct  $d_{x^2-y^2}$  symmetry by replacing the “bare” electron annihilation operators by the “quasiparticle operators” optimized for a single hole. They found that the trial wave function obtained in this way had a large overlap ( $\sim 90\%$  for  $t/J = 2.5$ ) with the exact two-hole ground state. This not only justifies our ansatz (16) for the two-hole ground-state wave function, but also provides evidence against the notion of some kind of “phase transition” that occurs when going from the undoped cluster to the cluster with two holes, which is suggested at least implicitly in Ref. 9.

(g) It has been shown that all the results for the momentum distribution and the spectral function can be explained at least qualitatively but often also quantitatively by the string picture.

Quite generally our interpretation explains and unifies in a consistent way quite a number of exact diagonalization results.

## ACKNOWLEDGMENTS

It is a pleasure for us to acknowledge numerous instructive discussions with Professor P. Fulde, Dr. K. W. Becker, Dr. P. Horsch, and Dr. G. Khaliulin. This work was supported by the Bundesministerium für Forschung und Technologie under Contract No. 03FU2MPG6. P.W.

gratefully acknowledges financial support from the IN-TiBS PAN statute program.

### APPENDIX A

The first problem in evaluating the momentum distribution is the calculation of the norm of the wave function  $|\Psi_d\rangle$  [see (16)]. This can be done using the formalism outlined in Ref. 27 and one finds that

$$n = \langle \Psi_d | \Psi_d \rangle = 1 - 2\tilde{n}_1 + 2\tilde{n}_2, \quad (\text{A1})$$

where  $\tilde{n}_1, \tilde{n}_2$  are defined in Ref. 27.

Next it is easy to see that there is a trivial contribution to the momentum distribution, which can be obtained by always taking  $j = j'$ . This then means that one is simply counting the number of spin- $\sigma$  electrons, and the result is of course  $\frac{1}{2} - \frac{1}{N}$  for each spin and each  $\mathbf{k}$ . In order to obtain nontrivial contributions the main problem is in finding all the combinations of sites such that the matrix element

$$\langle \Phi_{m',n'} | c_{j',\sigma}^\dagger c_{j,\sigma} | \Phi_{m,n} \rangle \quad (\text{A2})$$

is different from zero. In order to do the bookkeeping properly, we introduce the following graphical notation: we represent the states included in  $c_{j,\sigma} | \Phi_{m,n} \rangle$  by putting circles on the sites  $m$  and  $n$  and a square on the site  $j$ . The “track” of the holes is denoted by arrows. Similarly, the states in  $c_{j',\sigma} | \Phi_{m',n'} \rangle$  are represented by putting crosses onto the sites  $m'$  and  $n'$  and a diamond on  $j'$ . Then, each time the spin configurations and the positions of the holes in the two graphs match, we obtain a nonvanishing contribution. To assign a numerical value one has to bear in mind that a configuration where the first hole has hopped  $\mu$  times and the second hole  $\nu$  times has a prefactor of  $\alpha_{\mu,\nu} = \beta_{\mu,\nu} / (z-1)^{(\mu+\nu)/2}$ . In addition there may appear extra factors of  $(-1)$  which are either due to Fermi statistics or the extra factors of  $\epsilon_{m,n}$ . In order to assign the factors due to Fermi statistics properly, one has to bear in mind the following detail: by acting with the hopping term on the “initial state”  $\hat{c}_{m,\uparrow} \hat{c}_{n,\downarrow} | \Phi_{\text{Néel}} \rangle$  one obtains among other states,  $\hat{c}_{m,\downarrow}^\dagger \hat{c}_{l,\downarrow} \hat{c}_{m,\uparrow} \hat{c}_{n,\downarrow} | \Phi_{\text{Néel}} \rangle = -\hat{c}_{l,\downarrow} \hat{c}_{n,\downarrow} S_m^- | \Phi_{\text{Néel}} \rangle$ . Thus, the “double-string states” actually have additional prefactors of  $(-1)$  whenever the length of the string is odd. These extra factors have to be taken into account.

All in all we will obtain a representation of the spin-summed momentum distribution  $n_{\mathbf{k}}$  in the following form:

$$n_{\mathbf{k}} = \frac{1}{2} - \frac{1}{N} + \frac{1}{n} \sum_i n^{(i)}, \quad (\text{A3})$$

where  $n$  is defined in (A1). The simplest graphs (i.e., the ones involving the shortest strings) corresponding to each type of contribution are shown in Figs. 15, 16, and 17. The corresponding expressions are listed in Tables I, III, and IV. It should be noted, that the contribution  $n^{(1)}$  has already been discussed in the main text. For the sake of completeness it has been listed a second time here.

### APPENDIX B

In this appendix the calculation of the dispersion relation from the ansatz (32) will be sketched. In order to evaluate the expectation value of the Hamiltonian one needs to know matrix elements such as  $\langle \Phi_j^{(\mu)} | H | \Phi_i^{(\nu)} \rangle$  and overlap integrals such as  $\langle \Phi_j^{(\mu)} | \Phi_i^{(\nu)} \rangle$ . As has been discussed in Sec. II, in a Néel-ordered spin background there are two ways in which a hole can delocalize: by the string-truncation process, where the transverse part of the Heisenberg exchange repairs the defects created by the hopping hole and by hopping along a spiral path as first discussed by Brinkman and Rice.<sup>13</sup> In order to treat this second way of delocalization, one has to go beyond the retracable path approximation<sup>13</sup> and it has been demonstrated in Ref. 14 that this can be achieved via the definition of “irreducible paths.” Thereby a state obtained by creating a hole at some site  $j$  and acting on it repeatedly with the hopping term is called an “irreducible path with starting point  $j$ ” if it is not possible to generate the same state with fewer hops starting from a state where the hole was created at another site than  $j$ . This definition is illustrated in Fig. 14. In the following we assume that the summation over paths in (29) is restricted to irreducible states with starting point  $j$ . It will be assumed, however, that the use of the function  $\tilde{\beta}$  obtained by solving (30) remains a good approximation.

Let us first evaluate the matrix elements of the spin flip term  $H_1 = \sum_{\langle i,j \rangle} \frac{J}{2} (S_i^+ S_j^- + S_i^- S_j^+)$ . Consider the state shown in Fig. 13(a). In the state  $|\Phi_j^{(1)}\rangle$  it has expansion

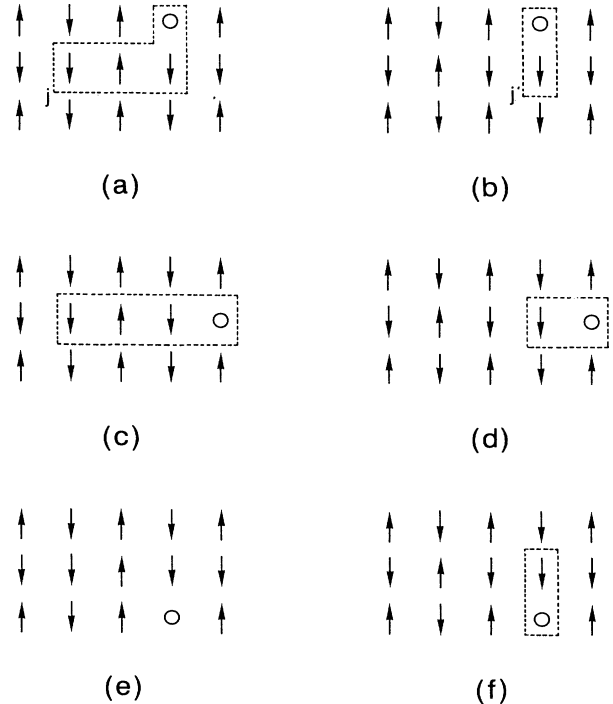


FIG. 13. Some processes that contribute to the matrix element  $\langle \Phi_{j'}^{(\mu)} | H_1 | \Phi_j^{(\nu)} \rangle$ .

coefficient  $\tilde{\alpha}_3$ . By acting with  $H_1$  it can be transformed into the state in 13(b). This one has expansion coefficient  $-\tilde{\alpha}_1$  in the state  $|\Phi_{j'}^{(1)}\rangle$  [the minus sign is due to the phase factor  $\phi_1(\mathcal{P})$ ]. Thus from this transition one gets a contribution of  $-\frac{J}{2}\tilde{\alpha}_1\tilde{\alpha}_3$ . By evaluating the contributions from the transitions Figs. 10(c)–10(d) and Figs. 10(e)–10(f) (thereby paying attention to the extra phase factors due to the geometry of the paths) and summing everything up one finds a total contribution of  $-\frac{J}{2}\tilde{\alpha}_1\tilde{\alpha}_3$ . This can also be generalized to longer paths and the whole procedure can also be repeated to obtain all matrix elements of the spin-flip term. One obtains ( $j$  and  $j'$  are second-nearest neighbors and  $j$  and  $j''$  are third-nearest neighbors)

$$\begin{aligned}
\langle \Phi_{j'}^{(1)} | H_1 | \Phi_j^{(1)} \rangle &= 2\tilde{h}_1 \\
\langle \Phi_{j''}^{(1)} | H_1 | \Phi_j^{(1)} \rangle &= -\tilde{h}_1, \\
\langle \Phi_{j+\hat{x}+\hat{y}}^{(2)} | H_1 | \Phi_j^{(2)} \rangle &= \langle \Phi_{j-\hat{x}-\hat{y}}^{(2)} | H_1 | \Phi_j^{(2)} \rangle = -2\tilde{h}_1, \\
\langle \Phi_{j+\hat{x}-\hat{y}}^{(2)} | H_1 | \Phi_j^{(2)} \rangle &= \langle \Phi_{j-\hat{x}+\hat{y}}^{(2)} | H_1 | \Phi_j^{(2)} \rangle = 2\tilde{h}_1, \\
\langle \Phi_{j''}^{(2)} | H_1 | \Phi_j^{(2)} \rangle &= \tilde{h}_1, \\
\langle \Phi_{j+\hat{x}-\hat{y}}^{(1)} | H_1 | \Phi_j^{(2)} \rangle &= \langle \Phi_{j-\hat{x}+\hat{y}}^{(1)} | H_1 | \Phi_j^{(2)} \rangle = 0, \\
\langle \Phi_{j+\hat{x}+\hat{y}}^{(1)} | H_1 | \Phi_j^{(2)} \rangle &= -\langle \Phi_{j-\hat{x}-\hat{y}}^{(1)} | H_1 | \Phi_j^{(2)} \rangle = -2\tilde{h}_1, \\
\langle \Phi_{j+2\hat{x}}^{(1)} | H_1 | \Phi_j^{(2)} \rangle &= \langle \Phi_{j+2\hat{y}}^{(1)} | H_1 | \Phi_j^{(2)} \rangle = \tilde{h}_1, \\
\langle \Phi_{j-2\hat{x}}^{(1)} | H_1 | \Phi_j^{(2)} \rangle &= \langle \Phi_{j-2\hat{y}}^{(1)} | H_1 | \Phi_j^{(2)} \rangle = -\tilde{h}_1, \\
\tilde{h}_1 &= \frac{J}{(z-1)^2} \sum_{\nu=1}^{\infty} \tilde{\beta}_{\nu} \tilde{\beta}_{\nu+2}.
\end{aligned} \tag{B1}$$

Next, let us turn to the matrix elements of the remaining term,  $H_0$ . To that end one can introduce the projection operator  $P_j$  which projects onto the subspace of irreducible paths with starting point  $j$  and its orthogonal complement  $Q_j = 1 - P_j$ . Then we have

$$\begin{aligned}
\langle \Phi_j^{(\mu)} | H_0 | \Phi_i^{(\nu)} \rangle &= \langle \Phi_j^{(\mu)} | P_j H_0 | \Phi_i^{(\nu)} \rangle + \langle \Phi_j^{(\mu)} | Q_j H_0 | \Phi_i^{(\nu)} \rangle \\
&= \tilde{E}_B \langle \Phi_j^{(\mu)} | \Phi_i^{(\nu)} \rangle + \langle \Phi_j^{(\mu)} | H_0 | \Phi_i^{(\nu)} \rangle, \tag{B2}
\end{aligned}$$

where in the second equation we used the fact that in the subspace of irreducible states with starting point  $i$   $|\Phi_i^{(\nu)}\rangle$  is an (approximate) eigenstate with eigenvalue  $\tilde{E}_B$ . In the second term only those hopping processes will contribute, where the hole is hopping “out of the subspace” of irreducible paths with starting point  $i$ . One example is the transition from the state shown in Fig. 14(b) to the one in 14(c). From this transition one will get a contribution which is equal to  $t\tilde{\alpha}_2\tilde{\alpha}_3$  (for  $\mu = \nu = 1$ ). Note that there is an additional factor  $(-1)$  due to the phase factors  $\phi_1(\mathcal{P})$ . Similarly one finds a contribution to the overlap of  $-\tilde{\alpha}_3^2$ . Generalizing these considerations one obtains the following matrix elements of the Hamiltonian:

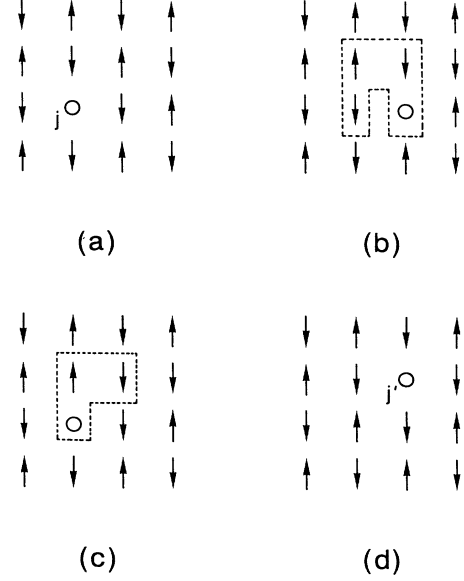


FIG. 14. Spiral path propagation mechanism for the hole. Starting from the state in (a) the one in (b) is obtained by three hops. One more hop leads to the one in (c), two more hops give the one in (d). The state (c) can be obtained with four hops from the one in (a) but with only two hops from the one in (d). Therefore it is not an “irreducible path with starting point  $j$  and is not included in  $|\Phi_j\rangle$ . The state in (c) can be obtained by three hops from both the state in (a) and the one in (d) and is therefore included into both  $|\Phi_j\rangle$  and  $|\Phi_{j'}\rangle$ .

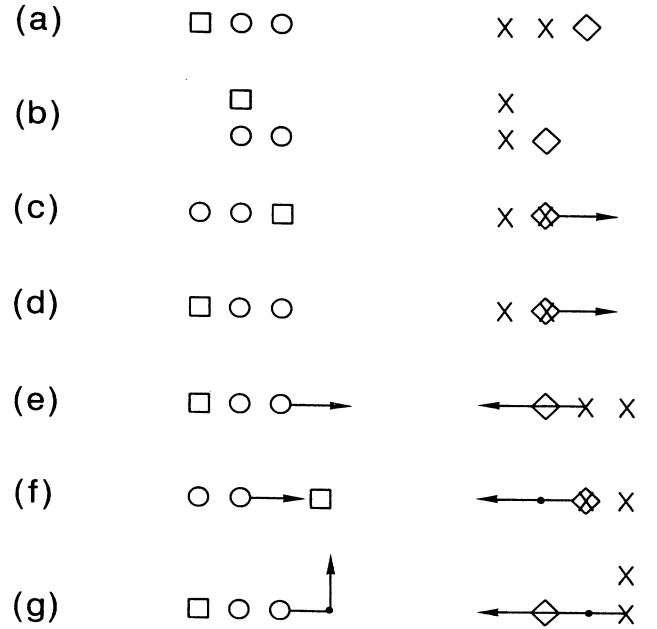


FIG. 15. Some processes that contribute to the momentum distribution.

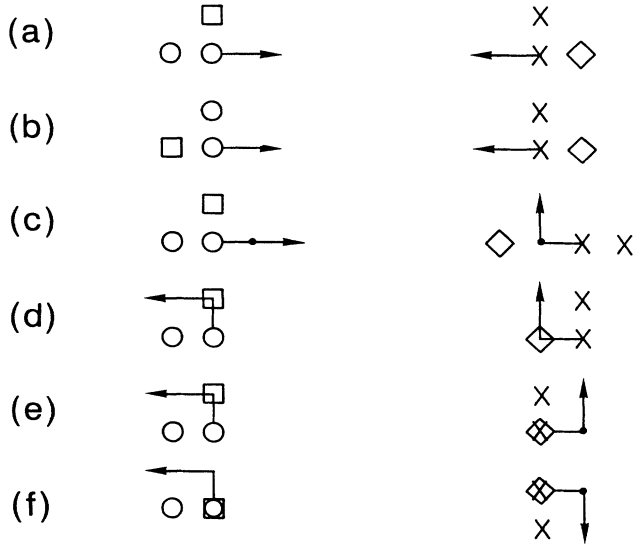


FIG. 16. Some processes that contribute to the momentum distribution.

$$\begin{aligned}
 \langle \Phi_{j'}^{(1)} | Q_j H_t | \Phi_j^{(1)} \rangle &= \tilde{h}_2, \\
 \langle \Phi_{j+\hat{x}+\hat{y}}^{(2)} | Q_j H_t | \Phi_j^{(2)} \rangle &= \langle \Phi_{j-\hat{x}-\hat{y}}^{(2)} | Q_j H_t | \Phi_j^{(2)} \rangle = -\tilde{h}_2, \\
 \langle \Phi_{j+\hat{x}-\hat{y}}^{(2)} | Q_j H_t | \Phi_j^{(2)} \rangle &= \langle \Phi_{j-\hat{x}+\hat{y}}^{(2)} | Q_j H_t | \Phi_j^{(2)} \rangle = \tilde{h}_2, \quad (\text{B3}) \\
 \langle \Phi_{j+\hat{x}-\hat{y}}^{(1)} | Q_j H_t | \Phi_j^{(2)} \rangle &= \langle \Phi_{j-\hat{x}+\hat{y}}^{(1)} | Q_j H_t | \Phi_j^{(2)} \rangle = 0, \\
 \langle \Phi_{j+\hat{x}+\hat{y}}^{(1)} | Q_j H_t | \Phi_j^{(2)} \rangle &= -\langle \Phi_{j-\hat{x}-\hat{y}}^{(1)} | Q_j H_t | \Phi_j^{(2)} \rangle = -\tilde{h}_2, \\
 \tilde{h}_2 &= 2t\tilde{\alpha}_2\tilde{\alpha}_3.
 \end{aligned}$$

Inserting the ansatz (32) one finds that for a wave vector

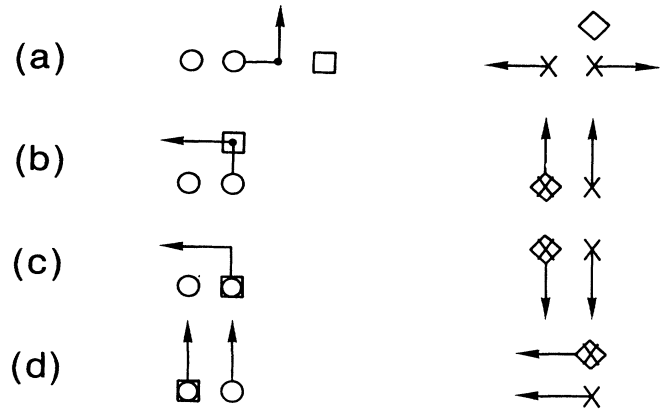


FIG. 17. Some processes that contribute to the momentum distribution.

$(k, k)$  the Hamilton matrix reads

$$H(k) = 4\tilde{h}_1 + 2\tilde{h}_2 + 2\tilde{h}_2 \cdot \begin{pmatrix} \cos(2k), & -i \sin(2k) \\ i \sin(2k), & -\cos(2k) \end{pmatrix}. \quad (\text{B4})$$

The overlap matrix reads

$$N(k) = 1 + 2\tilde{n} + 2\tilde{n} \cdot \begin{pmatrix} \cos(2k), & -i \sin(2k) \\ i \sin(2k), & -\cos(2k) \end{pmatrix}. \quad (\text{B5})$$

If one now assumes that the overlap integral  $\tilde{n}$  is small (this is confirmed by numerical evaluation), one can obtain the eigenvalues and eigenvectors simply by diagonalizing the matrix  $H$ . Then one obtains the expressions given in the main text.

\*Also at Institute for Low Temperature and Structure Research, P.O. Box 937, 50-950 Wrocław 2, Poland.  
<sup>1</sup>F. C. Zhang and T. M. Rice, Phys. Rev. B **37**, 3759 (1988).  
<sup>2</sup>S. Schmitt-Rink, C. M. Varma, and A. E. Ruckenstein, Phys. Rev. Lett. **60**, 2793 (1988).  
<sup>3</sup>C. L. Kane, P. A. Lee, and N. Read, Phys. Rev. B **39**, 6880 (1989).  
<sup>4</sup>S. A. Trugman, Phys. Rev. B **37**, 1597 (1988).  
<sup>5</sup>S. Maekawa, J. Inoue, and T. Tohyama; in *Strong Correlation and Superconductivity*, (Springer-Verlag, Berlin, 1989).  
<sup>6</sup>M. Grilli and G. Kotliar, Phys. Rev. Lett. **64**, 1170 (1990).  
<sup>7</sup>N. Nagaosa and P. A. Lee, Phys. Rev. Lett. **64**, 2450 (1990).  
<sup>8</sup>P. Prelovšek, I. Sega, and J. Bonča, Solid State Commun. **78**, 109 (1991).  
<sup>9</sup>W. Stephan and P. Horsch, Phys. Rev. Lett. **66**, 2258 (1991).  
<sup>10</sup>H. E. Castillo and C. A. Balseiro, Phys. Rev. Lett. **66**, 2258 (1991).  
<sup>11</sup>L. N. Bulaevskii, E. L. Nagaev, and D. L. Khomskii, Zh. Eksp. Teor. Fiz. **54**, 1562 (1968) [Sov. Phys. JETP **27**, 836

(1968)].  
<sup>12</sup>B. I. Shraiman and E. D. Siggia, Phys. Rev. Lett. **60**, 740 (1988).  
<sup>13</sup>W. F. Brinkman and T. M. Rice, Phys. Rev. B **2**, 1324 (1970).  
<sup>14</sup>R. Eder and K. W. Becker, Z. Phys. B **78**, 219 (1990).  
<sup>15</sup>K. v. Szczepanski, P. Horsch, W. Stephan, and M. Ziegler, Phys. Rev. B **41**, 2017 (1990).  
<sup>16</sup>V. Elser, D. A. Huse, B. I. Shraiman, and E. D. Siggia, Phys. Rev. B **41**, 6715 (1990).  
<sup>17</sup>J. Inoue and S. Maekawa, J. Phys. Soc. Jpn. **59**, 2110 (1990).  
<sup>18</sup>J. R. Schrieffer, X. G. Wen, S. C. Zhang, Phys. Rev. B **39**, 11663 (1989).  
<sup>19</sup>R. R. P. Singh and R. L. Glenister, Phys. Rev. B **46**, 14313 (1992).  
<sup>20</sup>A. Moreo, D. J. Scalapino, R. L. Sugar, S. R. White, and N. E. Bickers, Phys. Rev. B **41**, 2313 (1990).  
<sup>21</sup>R. Eder and K. W. Becker, Phys. Rev. B **42**, 4861 (1990).  
<sup>22</sup>Y. Hasegawa and D. Poilblanc, Phys. Rev. B **40**, 9035

- (1989).
- <sup>23</sup>P. Horsch and W. Stephan (unpublished).
- <sup>24</sup>E. Dagotto, J. Riera, and A. P. Young, Phys. Rev. B **42**, 2347 (1990).
- <sup>25</sup>J. Bonča, P. Prelovšek, and I. Sega, Phys. Rev. B **42**, 10 706 (1990).
- <sup>26</sup>P. Prelovšek, I. Sega, and J. Bonča, Phys. Rev. B **39**, 7074 (1989).
- <sup>27</sup>R. Eder, Phys. Rev. B **45**, 319 (1992).
- <sup>28</sup>E. Dagotto and J. R. Schrieffer, Phys. Rev. B **43**, 8705 (1991).
- <sup>29</sup>D. Poilblanc and E. Dagotto, Phys. Rev. B **42**, 4861 (1990).